ANALYSIS OF THE IMPACT OF USING GIS AND 2.5D MODELLING IN AUTOMATING THE DETERMINATION OF VIEW FACTORS FOR THE PURPOSES OF CAMA MODELLING.

JUSTINE KAHONDE

Thesis presented for the degree of Master of Science in Engineering

In the Department of Architecture, Planning and Geomatics

University of Cape Town

March 2006

DECLARATION

I hereby:

(a) grant the University free license to reproduce the above thesis in whole or in part, for the purpose of research.

(b) declare that:

i. I know the meaning of plagiarism and declare that all the work in the document, save for that which is properly acknowledged, is my own.

ii. neither the substance or any part of the thesis has been submitted in the past, or is being, or is to be submitted for a degree in the University or any other University.

iii. I am now presenting the thesis for examination for the Degree of Masters in Engineering.

Justine Kahonde **March 2006**

Signed by candidate

DEDICATION

"to my wife Callista, my parents, and my brothers and sister, I love you all. Thank you very much for your constant love"

ABSTRACT

Author: Justine Kahonde

Address: 3614 Tynwald North, West Gate, Harare, Zimbabwe

Thesis Title: Analysis of the Impact of using GIS and 2.5D modelling in automating the determination view factors for the purposes of CAMA modelling.

Date: March 2006

The main objective of this research is to investigate the impact of using GIS and 2.5D modelling in automating the process of determining view factors for CAMA modelling. Five metre contour data is used to generate digital terrain models (DTM) in the TIN data structure and in the raster data structure. The two terrain surfaces are assessed for accuracy by using Town Survey Marks (TSM) height data. It is found that the TIN surface models the terrain of the area under study more accurately than the raster method. This result is attributed to the fact that the TIN has the ability to accurately model mountainous surfaces by capturing peaks and pits better than the raster method. Buildings are modelled by extracting footprints off the aerial photographs, and they are converted into raster format so that they can be combined with the raster DTM. Two observers are simulated per building (one facing the ocean, and the other facing the mountain) and the viewshed analysis function is run to determine the visible areas. The views are grouped by type of view (mountain, ocean, other) and counting the number of visible cells per every observer. A *view index* (view factor) is generated for each building by dividing the number of visible cells by the number of visible cells of observers with the best view (beach front properties). The results of viewshed analysis show that the view was highly correlated with slope. In this regard, buildings high up on the mountain and those on the beachfront exhibit best views in terms of highest cell count, while those on the relatively flat areas exhibit poorest views. The view indices are then exported into NCSS software for CAMA analysis. The model for Quartile 4 used during the 2000 General Valuation is used for estimating property prices. The ratio analysis on the estimated prices with new view factors show that the results are less accurate than the ones generated during 2000 general valuation.

ACKNOWLEDGEMENTS

Ms Jenny Whittal:

Thank you very much for guiding me through the course of this study, and thank you very much for taking me on board. You have been there whenever I needed help. You have been a great supervisor.

Fellow Geomatics Postgraduates:

Thank you guys for everything. I really treasured you presence and your great contributions.

City Of Cape Town Valuation Management:

Many thanks go to Mr. Christopher Gavor and the entire management for allowing me to do my research and work with the CAMA team through this research.

Funding

This research was made possible through the financial support from the following organisations:

The University of Cape Town

The Lincoln Institute of Land Policy

The City Of Cape Town, Property Valuations Section

Table of Contents

List of Figures

List of Tables

List of Appendices

CHAPTER ONE: INTRODUCTION

1.0 Introduction

The metropolitan City of Cape Town is situated in one of the world's most stunning locations. Geographically, it is at the south-western most corner of the African continent with the Indian Ocean adjacent to it on the eastern side and on the western side one finds the Atlantic Ocean. Inland there is an array of great mountains among which one cannot miss the unique plateau of the Table Mountain and its attendant peaks- the Devil's Peak and the Lion's head. A combination of these mountains and the oceans create spectacular views from certain locations within the city. It is within these locations with great views of both the mountains and the oceans that one finds the most valuable and sought after properties. These properties are found mainly around the Table Mountain and the property market within these locations is very active. On the other hand the properties with the lowest market values are found in the low-lying flat areas where the views to the oceans and mountains are close to non-existent.

Figure 1.0: Ocean view

Figure 1.1: Mountain View

Figure 1.0 shows the view of the ocean as seen from one property in Sea Point area, while figure 1.1 shows the view of the Lion's head peak from the same property.

1.1 Background to the study

Computer Assisted Mass Appraisal (CAMA) is a systematic process of appraising a group of properties with similar characteristics at a given date using standardised procedures and statistical testing (Eckert, 1990). The metropolitan City of Cape Town's valuation department is in its early stages of using this method to appraise properties for taxation purposes. This system has a lot of challenges in its early stages of implementation in that it requires a team of highly specialised personnel, comprehensive system design, intensive data collection and analysis, model building and calibration, thorough analysis of results, and the generation of meaningful reports.

The successful implementation of this system relies in part on accurate input data. The collection of relevant property characteristics data is split into two categories: the land related characteristics data and the building related characteristics data. A mathematical model is then formulated based on these two categories with the aim of estimating the market value of a property in question from its characteristics data. Property characteristics such as the size of the living room, number of bedrooms, size of the stand, condition of buildings, and view are examples of the required data. While the determination of objective characteristics such as size of the living room and number of bedrooms is merely a straight forward process of measuring and counting, the collection of data about qualitative characteristics such as view is far more problematic. The process becomes challenging here because the data collector has to make subjective judgements about the quality of view and this depends much on his/her appreciation of that view.

1.2 Problem Statement

This research work draws its strength from the fact that the determination of view values for CAMA modelling by the City of Cape Town's valuation department is a bone of contention. View falls under the category of qualitative property data and as such its determination currently is by the use of inspection methods where a data collector goes and gives his/her judgement on the value of view. This kind of method is being criticised because of lack of consistency between data collectors and as such the City has attempted to improve the collection of view data by defining a broader category of view classes than the one used in GV2000.

The following section provides the view categories used during the GV2000 and the new proposed categories for the GV2006.

1.3 Current methods employed by the City to determine view

The method of collecting property view data used by the City during the 2000 General Valuation (GV2000) is explained below. View was categorised into a scale starting with excellent view at the top of the scale down to poor view at the bottom of the scale.
The following categories of view were extracted from the GV2000 data collection manual.

1. Excellent view is a superb unobstructed view of mountains, ocean, or vlei.

2. Above average view is a partially obstructed view of the mountain or ocean; distant unobstructed view of mountain, hillside or ocean. It is also a wide panoramic view from an elevated location.

3. An average view is a view typical of a neighbourhood position with no special view of the mountain or ocean.

4. Below average view is that of a commercial or industrial properties or non-residential area with no major detrimental effect on value.

5. A poor view is that of a heavy industrial area, railroad, rail yard, or major highways; view detrimental to property value.

The scale was revised for GV2006 as follows:

1. Excellent view represents a superb, clear, unobstructed view of the ocean from a reasonably short distance.

2. A panoramic view represents a distant, but clear, unobstructed view of one or more natural features (mountain or ocean). A panoramic view is typically a wide view from an elevated position. However, it also includes close, majestic views of the mountain.

In golf states, a clear view from a property overlooking a fairway would be included here.

3. Partially obstructed view represents an excellent or panoramic view as defined above, but with some obstruction of the view of the natural feature.

4. Above average view represents a limited view of one or more natural features. The view of the natural feature is normally distant or maybe within a few kilometres. The important point is that the view must be better than the average typical neighbourhood view and the natural feature is not spectacular e.g. a vlei.

5. Average view represents the typical neighbourhood position with no special view of any natural feature.

6. Below average view represents a view of one or more commercial or industrial properties or other feature that would detract from the normal average view. A view of a school would not be considered in this category.

7. Poor view represents a dominant view of a heavy industrial area, unattractive business areas, railroad, rail yard or major highway. Its effect is definitely detrimental to value.

The following problems were drawn from the analysis of the old method and the proposed scale for GV2006.

1. The inspection method is used in both cases and this method is subjective since it depends on the judgement of the data collector. Subjectivity in mass appraisal should be minimised so as to achieve the goal of equitable appraisal of properties.

2. Because the method involves data collectors going from property to property collecting the data, it can be very expensive as it requires a lot of personnel to cover a large jurisdiction like the City of Cape Town. A lot of time is also spent in data capture.

In light of the above mentioned problems it was therefore necessary to develop an objective method of collecting view data that is fast, more accurate, and cost effective.

1.4 Research Questions

1. What methods can one use to determine view for the purposes of CAMA modelling other than the inspection methods currently used by the City?

2. Can the process of determining view be automated in order to improve on efficiency of determination of the impact of view on property values, to reduce the element of subjectivity, and to improve the time and cost effectiveness of determining this characteristic?

3. Do the automated methods produce better models for the purposes of CAMA modelling?

1.5 Objectives

Primary objective

The primary objective of this research project is to develop an automated method of measuring view using GIS and 2.5D modelling which produces more accurate factors thereby eliminating the subjectivity associated with the current methods for the purposes of CAMA modelling.

Sub-objectives

1. To assess the accuracy of the view factors generated by the new method(s) by comparing the CAMA model with new view factors to the CAMA model with old view factors.
2. To contribute to the on going research on CAMA and GIS being undertaken internationally and at the University of Cape Town.

Hypotheses

Primary hypothesis

Geographic Information Systems (GIS) and 2.5-D modelling can be used in CAMA in order to develop an automated process of determining more accurate view data.

1.6 Research Method

Figure 1.2 illustrates the methods used in this research.

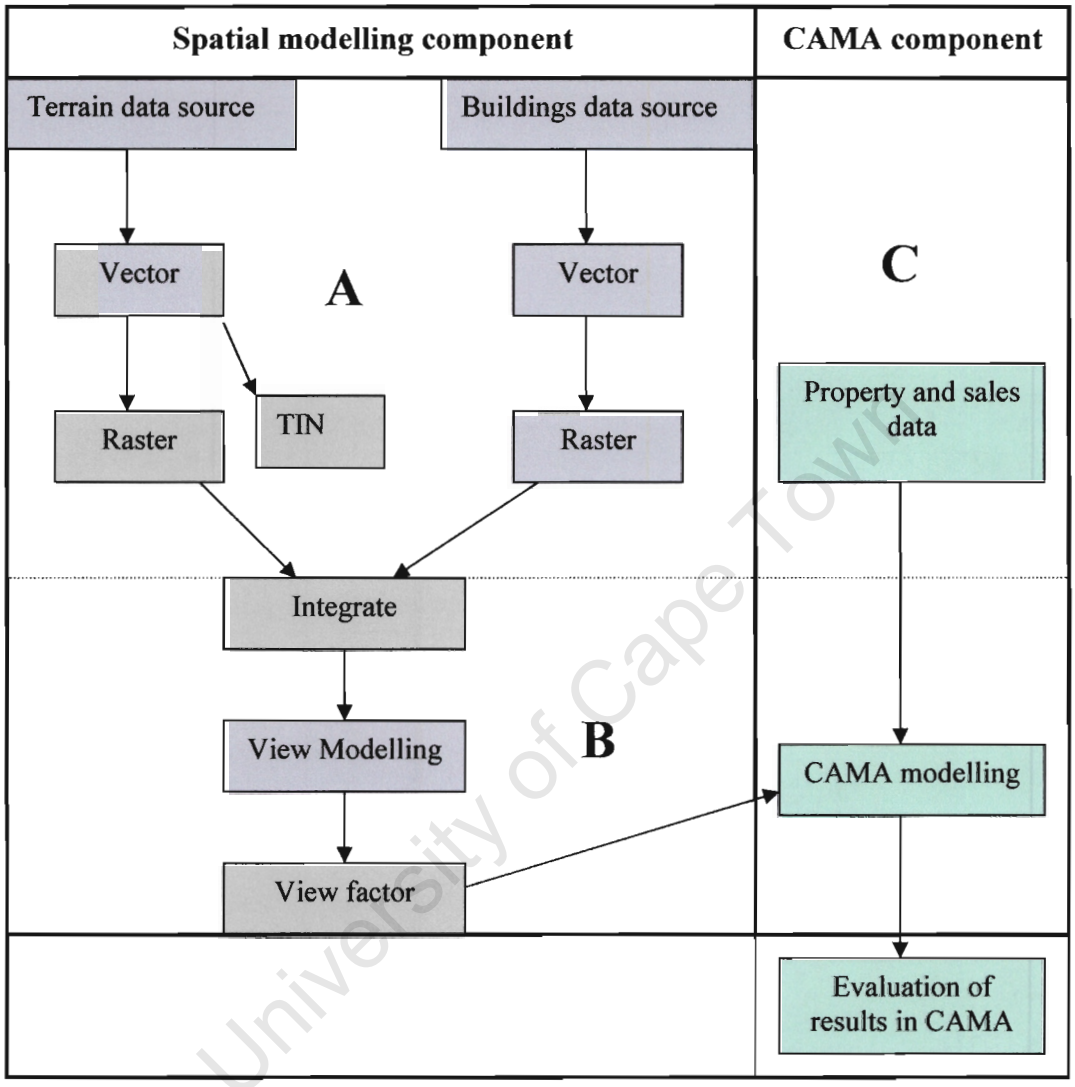

Figure 1.2: Research methods flow diagram

The research methods used in this research work can be classified under two broad areas: Spatial modelling and CAMA modelling as shown in figure 1.2. The aim of the spatial modelling component is to generate the view factors which will be imported into a CAMA system. In order to generate the view factors, a combined model of the earth and buildings is a prerequisite upon which view observations are made. To that effect, the process starts with spatial data collection where surface height data is collected and buildings data are captured as well.

The terrain height data is then converted into a surface to form a Digital Terrain Model (DTM) through the use of existing interpolation methods such as Triangulated Irregular Networks (TIN). On the other hand, the buildings vector data is converted into raster data format so that it can be combined with the DTM. A raster DTM is also produced so that the DTM can be combined with the buildings.

The raster buildings data and the raster DTM are then integrated to form one surface through the process of mathematical combination. Observers are then simulated on the DEM and the process of viewshed analysis is performed from which the view of the different buildings is determined. The results of this stage give the view factors which are exported into a CAMA system.

In the CAMA system, a model used by the City of Cape Town during the GV2000 is adopted and the view factors for the modelled properties are replaced with the factors generated from the new spatial method. The models are re-processed and the results tested by comparing the ratio analysis resulting from CAMA modelling with GV2000 view factors with the ratio analysis using new view factors.

1.7 Scope

View is treated in this work as it applies to CAMA property valuation systems. It is assumed that view is a significant factor affecting the value of properties and hence its use in the valuation models. The main focus here is to quantify view using the GIS methods.

The model developed in this work focuses on the quantification of ocean and mountain views, and this is based on the assumption that view varies with the extent of the ocean or mountain that is visible from the point of observation.

CAMA model development is not part of this research work. Hence, a model developed by the City of Cape Town will be adopted for testing the results.

The presence of trees is not considered in this research, based on the assumption that trees are not permanent features hence, their existence cannot be guaranteed. However, the modelling of trees as obstructions to view is recommended for further research. The different roof types are also not considered in this research work.

Software

For GIS analysis, the software ArcGIS 9 will be used. The software will be used because it is a commercial version and also because it contains all the necessary modules and extensions to perform the analytical operations. The software can also be customised to develop new applications using programming languages such as C++, or Visual Basic.Net. The software is also capable of handling large amounts of data and manipulating them in real time.

The Number Crunching Statistical Systems (NCSS) software will be used for running and testing the CAMA models. The software has the ability to handle fairly large amounts of data. However, for the purposes of this research work, the capacity of NCSS is deemed enough to test the model.

Hardware

A Pentium 4, 1 gigabyte ram, 3.2Hz processor desktop computer will be used in this research work.

1.8 Limitations

It was not possible to get hold of building outlines from the planning department. This was because of security reasons. Therefore, building outlines were estimated from an aerial photograph. The accuracy of the buildings model is thus affected.

Because of time constraints, a relatively small area is chosen as the case study. This is so as to allow for a comprehensive analysis of the method developed.

1.9 Structure of the thesis

In chapter two, the relevant literature dealing with recent research is reviewed. To that effect, methods of modelling view are reviewed with particular focus on property appraisal.

The third chapter explains the GIS theory used in this research work, while Chapter four focuses on the conceptual development of view model and the investigation into the different types of error that affect view for CAMA purposes.

The method of determining view developed in this work is explained in Chapter five.

Results and their analyses are discussed in Chapter six while Chapter seven gives the conclusions and recommendations.

CHAPTER TWO: LITERATURE REVIEW

In this chapter, literature relating to recent relevant research is reviewed. The chapter begins by reviewing research work that has primarily focused on modelling of view for the purposes of property valuations. Studies on other applications of view modelling are also reviewed. The reviewed literature shows that although the question of view has been studied by several researchers, there is no general agreement on the actual contribution view has on property values. It can be concluded that the value of view is thus dependent on locational factors. It is interesting to note that there has been a shift in the manner in which view is modeled due to technological advancements. Initially dummy variables were used, whereas in more recent studies researchers have attempted to use a 2.5D GIS modelling approach to view.

2.1 CAMA

Mass appraisal has been defined as the systematic appraisal of groups of properties as of a given date using standardised procedures and statistical testing (Eckert, 1990). In essence, CAMA is a relational database management and modelling system.

McCluskey and Borst (1997) makes it clear that the term mass appraisal by definition sets the parameters of the valuation context. CAMA is used to appraise a group of properties at a given time. A number of metropolitan cities have adopted this system. In their work, McCluskey and Borst (1997) describe how one can design an efficient and relevant mass appraisal. It is mentioned in their work that the currency, accuracy, and completeness of data are very important for mass appraisal. Because a lot of data about property characteristics is collected, the main strength of the CAMA system is in its ability to manage the data properly.

View is one of the main variables required by the CAMA system and as such, several studies have been undertaken to determine the value of view on property prices and these are discussed in the following section.

2.2 View and property valuations

Yu et al, (2004) reports that several studies have shown that views have a substantial impact on property values. However, there is no agreement on the actual contribution of view to the property values. The contribution varies from one market system to another.

Early studies on real estate valuation used single *dummy* variables to account for the view effect on property prices. Kulshreshtha and Gilles (1993) utilized dummy variables to estimate the value of a view of the South Saskatchewan River. It was later in 2001 when Seiler et al. (2001), found out that water views add substantial value to a property using dummy variables. Seiler et al, (2001) concluded from the analysis of appraisal-based data around Lake Erie that lake view adds 56% to home values. Bond et al., (2002) used a different method of transaction-based data around the same lake and found that lake view adds an 89.9% premium to a house.

Some studies have used several dummy variables to measure different types and qualities of views. Benson et al, (1998) examined the impact of views in Bellingham, Washington using dummy variables by splitting ocean view into four categories: full, superior, partial, good partial, and poor partial. They also used two levels for lake views: view from a lakefront property and view from a non-lakefront property, and whether or not the property has a mountain view. Bourassa et al., (2003) analysed the multi-dimensional feature of view by analysing the type of view, scope of view, distance to coast, and quality of the surrounding improvements. The impact of the views was empirically tested using dummy variables. The results indicated that aesthetic externalities have a substantial impact on residential property values.

However, in all these methods, view was determined by site inspection. Yu et al, (2004) reports that such a process can be very time consuming depending on the number of properties in a sample. In addition Yu et al., (2004) points out that the categorization of these views requires subjective interpretation that may not be consistent across properties or observers. Several researchers have suggested the use of GIS to obviate these shortcomings.

2.3 View modelling using GIS for property valuations

Lake et al, (1998) were among the first to utilize GIS to analyse the visibility of properties in Glasgow, Scotland. They used the viewshed function in GIS to calculate view scores based on what is visible from the property and then weight cells by their distance from the observer. In their analyses, buildings are considered as obstructions to view. Their results indicate that roads, railways and industrial estates have a negative impact on property prices.

Paterson and Boyle, (2002) used GIS data to develop variables representing the visibility of surrounding land use features in a hedonic model of suburban residential housing market. The visibility variables measured the percentage of the land visible overall within one kilometer of a property, as well as the percentage of visible land in each land use category. The results indicated that the visibility measures are important determinants of price and their exclusions may lead to incorrect conclusions regarding the significance and signs of other environmental variables.

Yu et al, (2004) employed a 3-D GIS approach to determine the impact of ocean views on property values in Singapore. They are perhaps the first to determine the extent of ocean views by calculating a view index. Because of the 3D approach used, they were able to simulate a potential development area and investigate the impact of ocean views on such an area. Their results show that ocean views add a premium of 15% to the property value.

2.4 Other GIS application areas of view analysis

According to Rana and Morley, (2002) visibility analysis has been applied successfully in a variety of applications which include planning of defense installations, landscape analysis, and environmental modelling.

Recent research on the use of GIS in view analysis has focused on optimizing visibility and improving the analysis. Rana and Morley, (2002) researched on the use a few observation points and targets to achieve the same results achieved in the traditional visibility analysis in GIS. Their work was driven by the fact that traditional visibility analysis in GIS takes a lot of time to compute. However, their study showed that by reducing the number of observers and targets, the accuracy is also reduced.

The ability of a GIS to extract features deemed important in a particular view is perhaps the driving factor in the use of GIS in view analysis. Baldwin et al, (1998) extracted the physical features affecting view and modeled the view by calculating a view index. In this study, the aim was to use GIS to model the environmental cognition of view. Thus, they attempted to model the effects of drama, mystery and coherence using a GIS.

In almost all the studies that have involved GIS in view analysis, a digital terrain model (DTM) has been the back bone of the method. Rana and Morley, (2002) generated a DTM upon which the viewshed analysis was performed. Yu et al, (2004) also generated a DTM which they overlaid with buildings to assess the view. All studies agree that errors in DTM need to be assessed as they affect the final product and in this case, they affect the view.

The viewshed operation found in most GIS software packages has been utilized by most researchers for visibility analysis. Yu et al, (2004) concluded that the viewshed operation has received considerable attention with respect to its operational reliability.

The literature has shown progression in the modelling of view for property valuations. It has shown first and foremost that view has an impact on the market values of properties however, the actual contribution of view is still a bone of contention among researchers. The use of GIS and a 3D approach which has been lately adopted by researchers shows a positive sign towards the modelling of view. However, the actual method of generating view indices has room for improvement.

This research work thus, builds on the strengths and the potential of using 3D GIS approach to model the view. However, the 3D GIS referred to in the literature is in fact 2.5D because the buildings are generated by extruding the building outlines by their heights. Therefore, the term 2.5D will be used in place of 3D in this research work.

CHAPTER THREE: GIS MODELLING AND CAMA ANALYSIS

In this chapter, the GIS techniques used in the development of view models and the CAMA analysis techniques used to test the view models are explained from a theoretical point of view. Central to the development of view models from a GIS perspective is a digital terrain model (DTM). Viewshed analysis is performed on the DTM to determine locations that are visible from a particular point of observation. From the viewshed analysis, the view can be quantified by way of counting the number of visible cells on the DTM. The view quantities are then linked to the CAMA models through a modelling procedure whereby the number of visible cells is converted to a view factor which is included in the model used to generate the market price of the property attributable to the view. To that effect, multiple regression analysis (MRA) techniques are utilised.

3.1 A Digital Terrain Model (DTM)

A DTM has been described as a particular form of computer surface modelling dealing with the specific problems of numerically representing the surface of the earth (Kennie and Petrie, 1990). It has also been defined as a *"statistical representation of the continuous surface of the ground by a large number of selected points with known X, Y, Z coordinates in an arbitrary coordinate field"*, (Naser, et al 2005). In essence, it is a digital representation of part of the earth's surface.

During the process of acquiring terrain data, a relatively unordered set of data elements is captured. In order to construct a comprehensive and usable DTM, it is necessary to establish topological relations between the data elements as well as an interpolation model to approximate the surface. There are several ways of representing the surface of the earth digitally. The surface model can be represented by contours which are polylines of constant height, regular grid height data (grid model) or by triangular surfaces known as triangular irregular networks (TIN). Regardless of surface model used, the following requirements are expected to be fulfilled by every surface model (ESRI, 1992). A surface model should:

1. Accurately represent the surface;
2. Be suitable for efficient data collection;
3. Minimise data storage requirements;
4. Maximise data modelling efficiency; and
5. Be suitable for surface analysis.

3.2 DTM generation

The generation of the DTM starts with data acquisition. Height data can be acquired by conventional methods which include ground survey, photogrammetric and cartographic methods. The ground survey methods are the most accurate but they are limited to small areas in terms of spatial coverage. The photogrammetric method utilises aerial photographs through the use of highly specialised equipment to extract height information from them. The cartographic methods involve scanning and digitisation of contour maps, which were most likely generated from aerial photogrammetric data originally. This is thus an indirect method of DTM generation and will include errors from both the photogrammetric and the scanning and digitising processes.

Advances in computer technology have seen the advent of new data acquisition methods which are both faster and more accurate than those mentioned above. These technologies include digital photogrammetry, airborne Light Detection and Ranging (LIDAR), Radio Detection and Ranging (RADAR), and ground based laser scanning systems.

3.2.1 Ground survey methods

Ground survey methods include the use of survey instruments such as the Global Position System (GPS) to measure three dimensional relative or absolute coordinates, total stations to measure distances and angles and levels to measure height differences. Surveys are usually limited in extent and concentrate on the special details of a specific site. Ground survey methods provide the most accurate data of height differences for terrain surface representation. However, due to the time and resource intensity of obtaining such data, ground survey methods are most often limited to small and accessible parts of the terrain. Only for high accuracy relative positions are ground survey methods used for large projects. These usually fall within the tasks of the national mapping authority in the establishment of vertical

and horizontal control networks for national mapping. Occasionally, however, they may be used for large construction projects such as tunnels.

3.2.3 Photogrammetric data capture

Photogrammetry has established itself as the main technique for obtaining precise 3-dimensional measurements from stereo-overlapped imagery (Hu et al., 1999). Conventional photogrammetry involves the use of expensive plotting equipment to mimic the stereo-geometry (stereo model) at the moment of image exposure. The processes involved in the development of the stereo model are the same in both conventional analogue and digital photogrammetry. The only difference is that for digital photogrammetry, the images are already in digital format and therefore ready for computer processing. The output from the photogrammetric process will generally be in the form of contours representing height differences, while plan positions of features will be indicated by points and lines.

3.2.2 Cartographic methods

Cartographic methods of acquiring height data for terrain surface modelling are scanning and digitizing of contour maps. The manual digitizing of maps is affected by the resolution of the map, the consistency of capturing of the data by the operator and the stability of the equipment used. The resolution of the map indicates the smallest detail that can be identified on the map. Higher accuracy is normally expected from a higher resolution map.

Automatic methods of extracting contours from the scanned maps exist. These methods utilize the concept of raster to vector conversion (R2V). With high resolution scanned maps, the R2V methods track contour lines to the resolution of the scanned map (Shears and Allan, 1996). R2V methods are more accurate and faster than manual cartographic methods. Cartographic methods have the major advantage over ground survey methods in that they benefit from the advantages of aerial photogrammetry in covering a much broader area and being more cost effective. However, the addition of sources of error from the photogrammetric process with those from the scanning and digitizing process should be clearly understood by the user, and the effects of these interpreted in the context of the required outputs.

Once the model has been produced, it is possible to extract the DTM through various sampling techniques which include regular sampling, progressive sampling, composite sampling and contouring. The aim of each of these methods is to minimize the data collection effort, while at the same time maximizing the accuracy of the resulting DTM.

Regular sampling- in this technique data is sampled at regular intervals either at the intersections of a regular square grid, at the apices of regular triangles or at the apices of any other regular polygon. Since a fixed sampling distance is used in these methods it is important to consider the determination of the optimal sampling interval.

Regular sampling has one major draw back in that the fixed sampling distance is not correlated with the amount of detail on the terrain. To that end, peculiar features such as peaks and pits/valleys may not be correctly sampled. On the other hand, the grid system may over sample surfaces that are generally of constant gradient. Thus, there is high risk of redundancy or under sampling when using this method.

Progressive sampling- with this method, the density of sample points is adapted to the complexity of the terrain surface. The sampling process begins by measuring a low density grid. The surface as represented by this grid is then assessed and areas of greater undulation are identified and measured using a denser grid. This is conducted progressively until the surface representation meets the required accuracy. A hierarchical sampling pattern results.

Composite sampling- in this method, selective sampling is used to capture special features such as peaks and pits/valleys while progressive sampling captures the data for the rest of the terrain.

Contouring- contours are systematically interpolated over the whole area of the model and an output of measurements in the form of strings of digital coordinates is produced.

3.2.4 Airborne LIDAR

LIDAR is an acronym for Light Detection And Ranging. It is sometimes also referred to as laser altimetry or airborne laser terrain mapping (ALTM) (Optech Inc, 2002). A LIDAR system consists of integration of three technologies; vertical laser distance measurement combined with positioning of the sensor using inertial navigation systems (INS) and GPS.

The elevation accuracy of LIDAR data is normally in the range of 15 – 25cm which makes it suitable for some applications that require accurate 3-dimensional data in urban areas, such as 3-D city modelling (Wehr and Lohr, 1999). LIDAR is highly cost effective because the processing sequence of the data can be largely automated from the acquisition in flight, through the evaluation, all the way to the end product of the elevation model (Naser et al, 2005).

3.2.5 Terrestrial laser scanning system

The laser scanning instrument sends a laser pulse with a known azimuth and vertical angle. The distance from the instrument is determined when the laser pulse is reflected back. The 3D coordinates for each point are then determined from the measured range (d), the horizontal direction and the vertical angle. Combined with the processing software, the system generates a data cloud so dense that it can resemble an image of the objects being mapped, however this varies with the scale of the image (Optech Inc, 2002).

3.2.6 RADAR based systems

RADAR stands for radio detection and ranging. Radio waves are considerably longer than those of visible light. A radar system consists of a transmitter, an antenna, and a receiver. The accuracy of RADAR is worst of all the methods, yielding 0.5m accuracy in heights.

Table 3.1: Data acquisition methods

	Ground survey	Aerial photography	LIDAR	LASER	RADAR
Accuracy	=<0.20m	1 – 2m	0.15- 0.25m	0.15-.25m	0.5m
Cost	Expensive	Relatively cost effective	Cost effective	Cost effective	Cost effective

3.3 DTM Data structures

A terrain surface can be represented as irregular points, contours, regular square grid or as a TIN model. Irregular points are rarely used to represent a surface because it is difficult to visualise the surface from this. On the other hand, contours are also stored as a string of points with constant height (z coordinate is a constant). The data models for the grid model and the TIN model are more complex than for the contours and the point data. These are dealt with in the following sections.

3.3.1 Data structures in grid models

Grid models are based on a very simple data structure which is comprised of a two-dimensional matrix of elevations, sampled at regular intervals in xy (horizontal) plane. It is fundamental to note that the grid structure is only representative of discrete points in the xy plane and is not a continuous surface.

The cell size inherently constrains the spatial resolution of a grid DTM. It therefore follows that the smaller the cell size, the higher the resolution, which is distinct from the quality of the original data, but is also limited by it.

DTM files are usually large, and therefore, minimising storage space is of utmost importance. Large data files often imply higher costs of maintenance, and more time in transmitting the data. To minimise the size of data stored, data compression can be used. Data compression works on the principle that data consisting of large homogeneous features can be compressed better than data consisting of small fragmented polygons. While some compression techniques compress some data better than others, no compression technique compresses all types of data more effectively than another (Samet, 1984). Two compression techniques are of utmost importance in grid data model:

- Run-length encoding
- Quad tree compression

Run-length encoding- the principle behind this technique is that adjacent cells along a row that have the same value are treated as a group termed a run. The value is stored once, together with information about the size and the location of the run. The value of the attribute, the number of the cells in the run, and the row number are recorded. Run length encoding

stores data by row. A row is first identified, followed by the columns and the value associated with the row-column location. The compression is "lossless" since the original data can be exactly reproduced. A major advantage of this technique is that it is very simple to implement (Naser et al, 2005).

DTM Data

1	2	3	4	5	6	7	8
15	15	15	15	16	16	17	17
15	15	16	16	16	16	17	17
15	16	16	16	17	17	17	17
16	16	16	17	17	17	17	17

Run-Length encoding

15,4,16,6,17,8

15,2,16,6,17,8

15,1,16,4,17,8

16.3.17.8

Quad tree- the quad tree data model provides a more compact raster representation by using a variable-sized grid cell. Finer subdivisions are only used in areas with finer detail. By conducting this form of compression, a higher level of resolution is provided only where it is needed.

The process typically begins by dividing a grid area into four equal, smaller squares when cells in the grid have different values. If all the cells within any of the four smaller squares have the same value, the square will not be broken down any further. However, if there are cells with different values, that square has to be subdivided into four more equal squares. The process continues until each square only represents cells with the same values (Chen and Tobler, 1986).

3.3.2 TIN model data structures

The TIN data structures are made of three geometric elements which are the *node*, the *edge*, and the *triangle* data structure.

Node-based data structure- each node data object includes (x,y,z) coordinates, the number of neighbouring nodes, and a pointer to one of its directed edges. The directed edges originate at the node (Tucker and Slingerland, 1997).

Triangle-based data structure- a triangle-based data structure is based on three tables (Bjorke, 1988):

- a point table containing x,y, and z coordinates
- an edge table with pointers to the end points and adjacent triangles of the edges, and
- a triangle table consisting of pointers to the edges that define the current triangle.

Edge-based data structures- in an edge-based data structure all information about the triangle is implicit in the edge table. Voronoi Diagrams (VD), and Delaunay Triangulation are both edge-based data structures.

Voronoi Diagrams (VD)

A voronoi diagram is a geometric structure that represents proximity information for a set of points. Given a set of points, a VD represents the regions of a plane that are closer to a particular point in the plane than to any other point (McCullagh and Ross, 1980). VDs are very useful in solving the nearest neighbour problem.

Delaunay Triangulation

Delaunay triangulation and Voronoi diagrams are closely related. Delaunay triangulation is constructed by drawing lines between the points in adjacent polygons defined by the VD. When the construction is finished, a triangular network that covers the whole area is achieved.

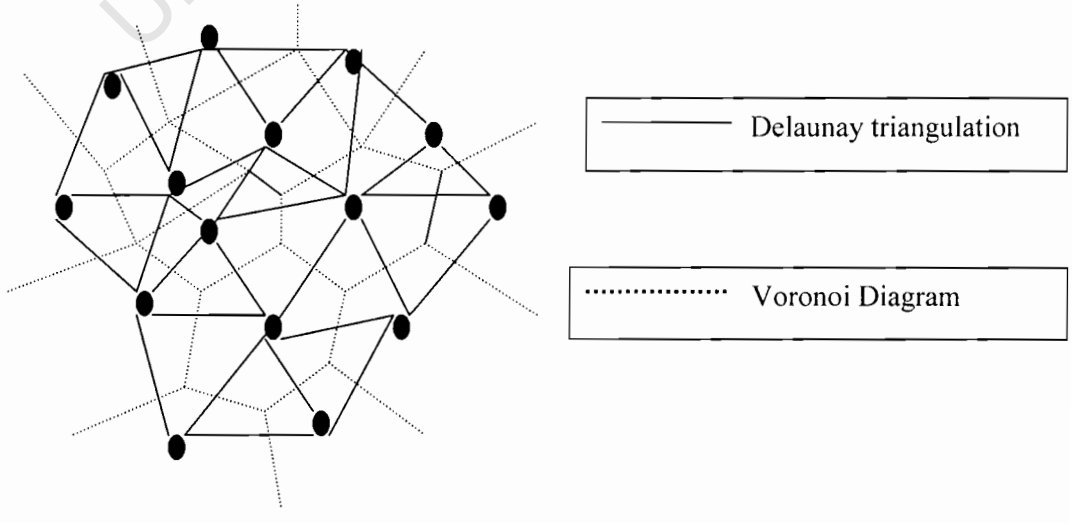

Figure 3.1 The relationship between a Voronoi diagram and the Delaunay triangulation

3.4 DTM interpolation

Naser et al., (2005) define interpolation as the process of estimating the value of attributes at some sites from measurements made at surrounding point locations, which are denoted as sample or reference points.

With regards to DTM interpolation, the following points are noteworthy (Naser et al., 2005):

1. There is no best interpolation algorithm that is clearly superior to all others and appropriate for all applications.
2. The quality of the resulting DTM is controlled by the distribution and accuracy of the original sample points as well as the adequacy of the underlying assumptions of the interpolation model.
3. The most important criterion for selecting a DTM interpolation method is the degree to which the key surface features can be taken into account and its capability in capturing varying terrain characteristic.

3.4.1 Classification of interpolation methods

Interpolation methods can be classified as exact methods versus inexact methods, global methods versus local method, or as stochastic methods versus deterministic methods (Bjorke, 1988).

Exact versus Inexact methods – an exact interpolation method generates a surface that passes through the sampled points. On the other hand, an inexact interpolation method yields different elevation values at the sampled points. The statistical differences between the given and interpolated elevations at the same points are often used as indicators of quality of an inexact interpolator.

Global versus local interpolation – global interpolation method uses all the available samples to estimate the elevation at the interpolation point. In contrast, local interpolation estimates the unknown elevation using sample points nearest to the interpolation point.

Stochastic versus deterministic interpolation – stochastic methods consider the statistical properties of the surface and the sampled elevations within the interpolation mechanism. On the other hand, deterministic methods do not consider the statistical properties of the surface and the sample elevations.

3.4.2 Global interpolation methods

The global interpolation methods that are used in many applications are the Trend Surface Analysis (TSA), Fourier Analysis (FA), and KRIGING. TSA is a deterministic interpolation, which approximates the surface by a polynomial expansion of the XY geographic coordinates (Davis, 1986). In principle, an observed elevation at a sampled point is considered to be the sum of a polynomial function of its XY-coordinates (trend) and a random error (residual). Fourier Analysis is used to decompose spatial or time-domain signals as the summation of scaled basis functions in the form of complex exponentials/sinusoidal waves with different frequencies (Jahne, 1997). On the other hand, Kriging is a geostatistical interpolation technique that estimates the elevation at the interpolation point as a weighted average of the observed elevations at the sampled points (Clark, 1979).

3.4.3 Local interpolation methods

Among the local interpolation techniques used, the nearest neighbour, linear interpolation, bilinear interpolation, cubic convolution, and the inverse distance weighting are the most commonly used (Jahne, 1997).

(a) **Nearest neighbour** – the nearest neighbour assigns the elevation associated with the closest sample point under consideration. There is no averaging of the elevations at neighbouring sample points. The major advantage of this technique is that is computationally efficient. However, the technique produces discontinuous surfaces.

(b) **Linear interpolation** – this technique uses the closest three sample points to define a planar surface. The fitted plane is then used to estimate the elevation at the interpolation point in question. The linear interpolation produces a continuous surface that passes through the sample points. It is an exact interpolator.

(c) Bilinear interpolation – a bilinear interpolation technique considers the whole grid element as the basic unit. It produces a continuous and non-smooth surface that passes through the sample points (i.e., exact interpolator). A bilinear polynomial is usually of the form:

$$Z(X,Y) = a_0 + a_1 X + a_2 Y + a_3 XY \qquad 3.1$$

where, a_0, a_1, a_2, and a_3 are the coefficients of the polynomial. Using four sample points at the corners of the grid element including the interpolation point, it is possible to define the four equations. These four equations can be used to evaluate the bilinear polynomial coefficients, which can be used to estimate the elevation at the interpolation point.

(d) Cubic convolution – cubic convolution calculates the output Z value as a weighted average of the elevations at the closest sixteen sample points.

(e) Inverse distance weighting (IDW) – IDW estimates the Z value at a point as a weighted average of the elevations at nearby sample points. The weights are inversely proportional to the distance between the interpolation point and the sample points in question. As a result, nearby points will have higher weight than more distant points. The weighting function and averaging process can be mathematically described by (3.2):

$$Z(X,Y) = \left[\sum_{i=1}^{n}\left[\frac{Z_i}{d_i^{\,p}}\right]\right] \Big/ \left[\sum_{i=1}^{n}\left[\frac{1}{d_i^{\,p}}\right]\right] \qquad 3.2$$

Where Z(X,Y), is the estimated Z value at the location (X,Y) while Z_i is the elevation at the i^{th} sample point located at (X_i,Y_i), d_i is the distance between the sample points and the interpolation points, and p is the power to which the distance is raised (Naser et al., 2005). If p=1, the function reduces to a simple linear interpolation between the points. According to Naser et al., (2005), p = 2 produces better results.

3.4.4 Interpolating grid from contours

If the measured terrain model data takes the form of contours, a different technique of interpolation must be used (Leberl and Olsen, 1982). In this case, a search is made along each of the four lines passing through the required grid node and oriented along the grid directions (VV and HH) and their bisectors (UU and GG) as shown in figure 3.2. The intersection of each of the eight directions with the nearest contours is established and the slope of each of the four lines calculated. The line with the steepest slope is then selected, and the value of the elevation of the grid node established by linear interpolation along this line (Kennie and Petrie, 1990).

If for instance, in figure 3.2 the line GG has the steepest slope, then the height of the grid node P is derived from equation 3.3.

$$H_P = [H_1 - H_5] * \left[\frac{d_{P5}}{d_{15}} \right] + H_5 \qquad (3.3)$$

Where H_1 and H_5 are the heights of points 1 and 5 respectively, and d_{P5} and d_{15} are the distances between points P and 5, and points 1 and 5 respectively.

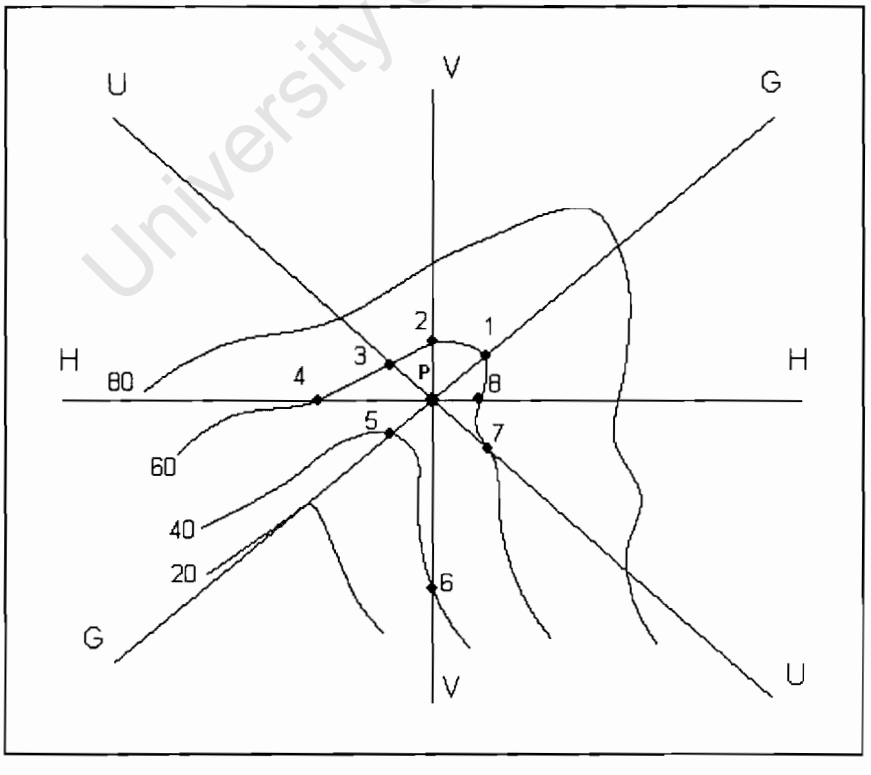

Figure 3.2: Sequential steepest slope algorithm showing cross-sections HH, VV, UU, and GG, and the intersection points on the contours (Leberl and Olsen, 1982)

3.5 DTM quality control

The accuracy of a DTM can be assessed by comparing the DTM to another DTM of higher accuracy for the same area. In this case, the first DTM is interpolated to produce data points coinciding with the points in the second DTM. The elevations at corresponding points are then compared to provide a quantitative measure of the differences between the two data sets (Naser et al., 2005).

3.6 Viewshed Analysis

Viewshed operations are traditionally performed on terrain surfaces (Yu et al, 2004). In principle the concept of viewshed is used to determine a set of visible points from a particular point of observation. A viewshed map is generated as a map showing the areas that are visible and those that are not visible from the point of observation.

The principle behind viewshed is illustrated in figure 3.3. Two points V and W on a topographic surface are said to be mutually visible if and only if the interior of the straight line segment joining them lies strictly above the terrain. Such a segment is allowed to touch the surface at most at its end points V and W. Any point V lying on or above a topographic surface can be chosen as a viewpoint (Fisher, 1993).

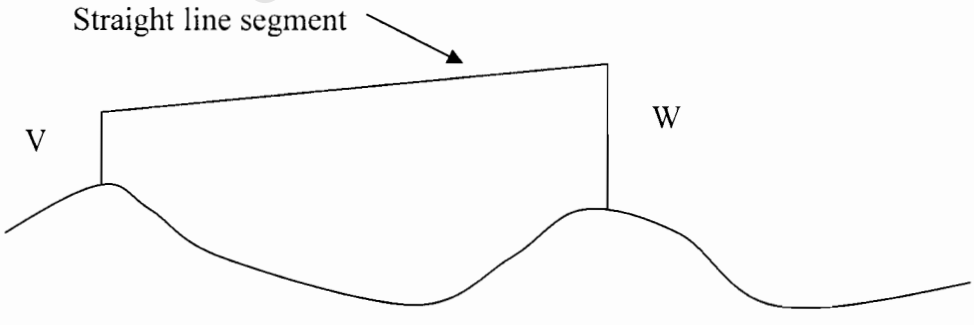

Figure 3.3: Visibility structure

Given a viewpoint V on a terrain, the viewshed of V is the set of points of the surface which are visible from V, that is;

$$viewshed(V) = \{W \in D \setminus W\} \text{ is visible from V} \qquad (3.4)$$

Where, W is the set of points in the domain D given that W is visible from V.

A viewshed map generated in the raster model is made up of 1's and 0's where 1's represent a visible cell and the 0's represent non-visible cells. This results in a binary model. It is thus possible to rank the different viewshed maps according to the number of the visible or non-visible cells (Yu et al, 2004).

3.7 Mass Appraisal and CAMA

This section attempts to give an overview of Mass Appraisal and CAMA systems. The aim is to familiarise the reader with the appraisal concepts.

CAMA has already been defined as a systematic process of appraising a group of homogeneous properties at a given date using standardised procedures and statistical analysis (Eckert, 1990). Traditionally, the appraisal of properties was performed on a single property basis. Such a procedure is known as the single-property appraisal. Although the use of single-property appraisal is still in use, most organisations have limited its use to special purpose appraisals such as appeals or sales (Gloudemans, 1999).

Mass appraisal and single-appraisal differ in the method of market analysis and quality control. For mass appraisals, models are formulated and a group of properties is passed for valuation at the same time while for single property appraisal, only one property is appraised at a time. Quality control is handled differently in both cases. Statistical analysis is used to evaluate the accuracy of mass appraisals while for single appraisal, similar properties which have sold are used as the bench marks for the value of the appraised property. Since CAMA attempts to value a large number of properties simultaneously involving large quantities of data, it requires a team of skilled personnel to work at the same time whereas for single appraisal only one person is required. As a result, CAMA is preferred to single-property

appraisal because organisations are able to meet deadlines and thus cut down on otherwise high costs and time consuming processes (Ward, 2001).

3.7.1 Comparable Sales Approach

The comparable sales approach is one of the techniques used to appraise properties. The other techniques are:

- Cost Approach
- Income Capitalisation Approach.

All the three techniques are closely related and any one of them can be used during the appraisal process with the most accurate appraisal of property achieved if all techniques are used in the analysis.

The comparable sales approach is based on the assumption that a buyer is well informed of how the property market operates and that the price paid for purchasing a certain property is a good estimate of the market value, and as such indicates the price of acquiring a comparable one in the same market (French et al., 2003). The appraiser compares the property of interest to other similar sold properties; rarely will two properties be identical in terms of property characteristics hence the need to adjust the sale prices of the sold properties. Once the sale prices of the comparable properties have been adjusted they are then summed up and an average value determined which corresponds to the market value estimate of the property of interest. This approach is mainly used for single-residential valuations but the major disadvantage is that if comparable sales are very few, it is difficult to generate an acceptable estimate.

3.7.2 Property data

Data could be defined as codes, words, numbers or symbols that have been observed or measured in a sequential manner (Gloudemans, 1999). Property data types fall into two major categories which are *qualitative* data and *quantitative* data. Qualitative data are non-numeric, this means that they tend to be discreet. Examples of qualitative variables are the condition of a property, quality and view. On the other hand quantitative variables are measurable and these include the size of the living room, the number of bedrooms among others.

3.7.3 Modelling

A model is a representation of the relationship between various elements of a real situation and it is used to test theories or predict outcomes of events (Eckert, 1990). A model consists of a dependent variable and at least one independent variable. In the case of CAMA, the dependent variable is the sale price (SP) of real property, while the independent variables are the property characteristics. In CAMA, regression models are used to estimate the market value of real property.

3.7.4 Multiple Regression Analysis (MRA)

Multiple Regression Analysis (MRA) is a statistical technique for estimating market values using the sale price and property characteristics (Eckert, 1990). The contribution of each variable to the market value of a property is reflected by its coefficient which is derived from sales analysis. The aim of MRA in mass appraisal is to model the relationship between property characteristics and market value.

3.7.5 Evaluation of CAMA results

Statistical methods are used to evaluate the CAMA performance. In this case the aim is to statistically analyse the estimated selling prices of properties against the actual sale prices. *Ratio studies* are the main tools used in the analysis of CAMA results (Eckert, 1990). The sales ratio is computed by dividing the estimated sale price by the actual sale price. Goodness of fit statistics are used to assess the predictive accuracy of the model. These are the Coefficient of Determination *(R^2)*, standard error of estimate *(see)*, Coefficient of variation *(CoV)*, and the average percent error.

Coefficient of Determination *(R^2)*

The coefficient of determination *(R^2)* is the percentage of the variation in sales prices explained by the regression model (Gloudemans, 1999). R^2 ranges from zero to one. When it is equal to zero, it means that none of the variation is explained by the regression model, and when it is equal to one, it means all the variation is explained by the model i.e., the variation

is due to the independent variables. For properties that have sold, the sum of the squared errors (SSE) associated with this estimate is:

$$SSE = \sum \left(S_i - \overline{S}\right)^2 \qquad 3.5$$

where,

S_i is the sale price of property i

$\overline{S}$ is the average sale price and,

$i = 1, 2, \ldots, n$ (where n is the number of sales).

The sum of the squared errors of the regression model (SSE_{UN}) is the statistic;

$$SSE_{UN} = \sum e_i^{\,2} = \sum \left(S_i - \hat{S}\right) \qquad 3.6$$

where $\hat{S}$ is the estimated sale price.

Now R^2 is given by:

$$R^2 = 1 - SSE_{UN} / SSE \qquad 3.7$$

Making substitutions for SSE_{UN} and SSE given in equation 1.1 and 1.2 respectively equation 1.3 gives:

$$R^2 = \sum \left(\hat{S}_i - \overline{S}\right)^2 / \sum \left(S_i - \overline{S}\right)^2 \qquad 3.8$$

The shortcoming of R^2 is due to the fact that as more regression variables are added, R^2 can only increase or stay the same which can overstate the goodness of fit when insignificant variables are included or when the number of variables is large relative to the number of sales (Ward, 2001).

In order to counter the shortcoming of R^2, its sister statistic represented by $\overline{R^2}$ is used and it is given by the following equation:

$$\overline{R^2} = 1 - \left[(n-1)SSE_{UN} / (n-p-1)SSE\right] \qquad 3.9$$

where n is the sample size and p is the number of regression variables.

Standard Error of Estimate (see)

The standard error of the estimate *(see)* is the measure of the amount of deviation between the sale price and the estimated market value (Eckert, 1990). *see* is given by:

$$see = \left[\sum \left(S_i - \hat{S}_i \right)^2 / (n - p - 1) \right]^{1/2} \qquad 3.10$$

Calculation of *see* is analogous to the calculation of the standard deviation. This implies that if errors are normally distributed, then the following holds:

- 66% of the sale prices will fall within one *see* of their estimated values
- 95% of the sale prices will fall within two *see* of their estimated values
- 99% of the sale prices will fall within three *see* of their estimated values

This method is however affected by outliers as they tend to affect the mean sale price.

Coefficient of Variation (CoV)

CoV is *see* expressed as a percentage of the average sale price and multiplied by 100:

$$CoV = (100 * see / \overline{S}) \qquad 3.11$$

The interpretation of *CoV* rests on the assumption of normal distribution of errors and when the normality assumption is met, *CoV* proves to be a powerful measure of uniformity. However, when there is no normality, *CoV* can be a misleading gauge of uniformity. The following relationships hold for *CoV*;

CoV	**Percent of ratios**
±1	68
±2	95
±3	99

CHAPTER FOUR: MODEL BUILDING CONCEPTUAL DESIGN

The GIS concepts explained in chapter three are used to conceptually build the view model in this chapter. Since the aim of this research work is to design a method of determining the view factors for the purposes of CAMA modelling using GIS modelling techniques, this chapter focuses on the conceptual design of the method by explaining the stages involved and methods of analysing the errors introduced during each stage. First the DTM design is explained, followed by the design of the building models. The method of generating a combined model of the terrain and the buildings is then explained together with the possible errors inherent in the methods used. Finally, the method of carrying out viewshed analysis is explained. The flow diagram shown in figure 4.1 gives an outline of the stages involved in the design process.

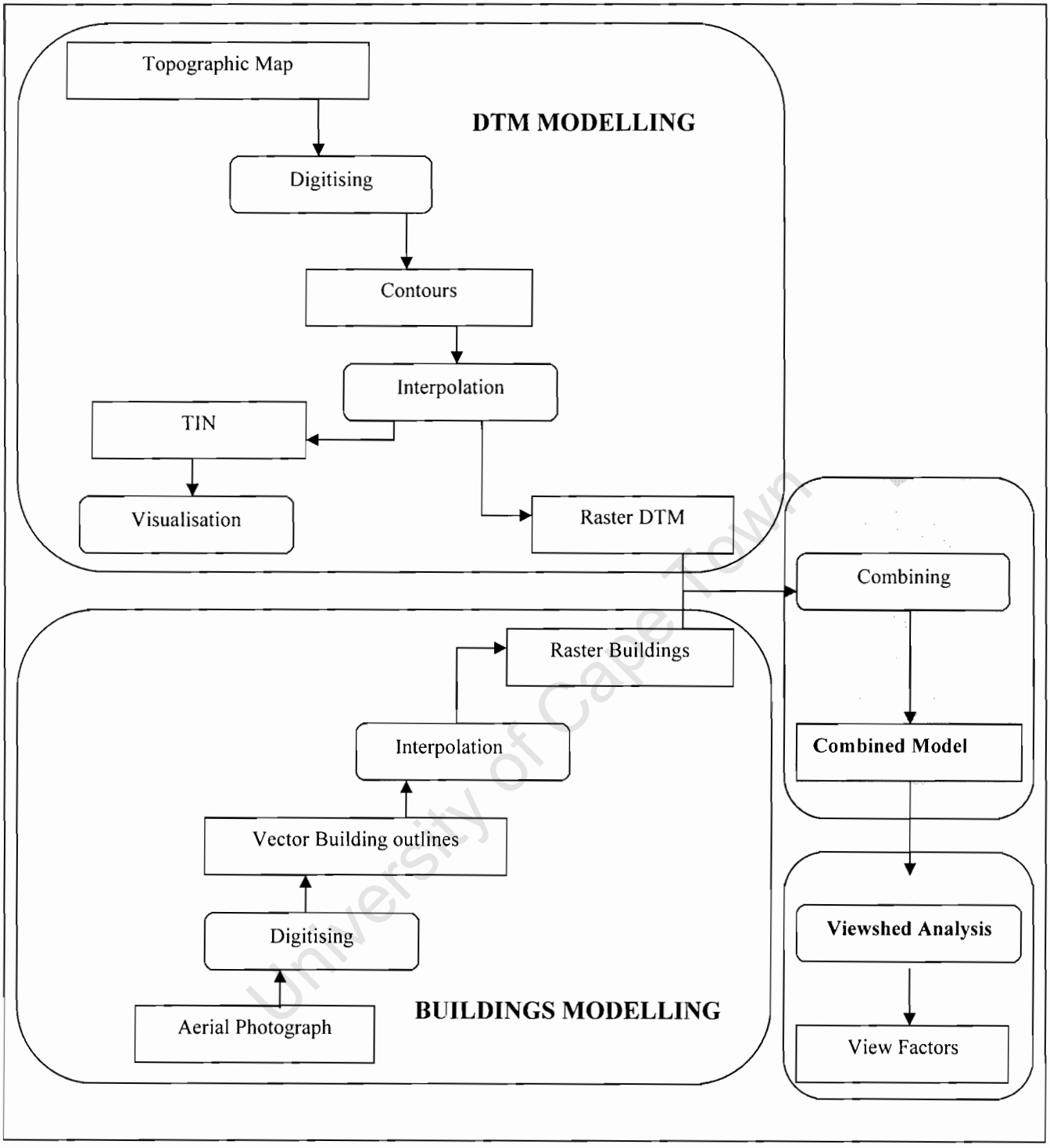

Figure 4.1 Conceptual Flow diagram of view modelling

The process of modelling view is split into four major categories which are; DTM generation, Buildings modelling, the combination of the two models, and the viewshed analysis.

4.1 DTM generation

As depicted by figure 4.1, the design of a DTM for the purposes of modelling of view for CAMA valuations involves a couple of stages. These stages are the digitisation of height data from a topographic map, and the interpolation of TIN and raster DTM from the contour data. Numerous errors are introduced in each method used during the process and as such it is of paramount importance that the effect of these errors be understood.

4.1.1 Digitisation of contour data

The method of digitising contours as the source of height data from a topographic map is proposed for this research work. The method of contours has a number of advantages which include among others, the ability to model a large area depending on the scale of the map, and the possibility of generating the DTM using a variety of interpolation techniques as explained in chapter three. However, it has the major disadvantage that the contours on the map were originally interpolated from other height data and to that effect errors in the original interpolation are carried forward. These are then compounded with the expected human errors inherent in the digitising process. Despite the disadvantages of the contour method over other methods explained in chapter three, the digitisation of the contours is used in this work for two major reasons:

- Topographic maps are easily available and the digitisation procedure can be readily performed on desktop computers using common software such as the ArcGIS. This in fact has the advantage of reducing the costs involved with data acquisition through specialised techniques such as photogrammetry and laser technology.

- The second reason follows from the first in that the view model produced in this case can be assessed to ascertain whether its inclusion in the CAMA model yields market value estimates according to International Association of Assessing Officers (IAAO) standards.

4.1.2 DTM Interpolation

The contours so produced are then used to interpolate the DTM. Both the TIN and the raster DTM are interpolated. The TIN is interpolated for the purposes of visualisation. This is because the TIN

gives the perspective view of the terrain which may be of great significance for the purposes of defending the values generated by the CAMA process when these values are appealed by the property tax paying public. On the other hand, the raster DTM is used for the modelling of the combined model of buildings and the terrain. Since the raster DTM is made up of cells it is possible to apply arithmetic operations on it which facilitates combining the models.

As explained in Chapter Three, the TIN method is preferred as it honours the data points used in the field. This results from its ability to model, without interpolation, features such as mountain peaks and valleys, hence its ability to generate a perspective model of the terrain. The accuracy of the TIN depends on the accuracy of the field data and on the accuracy of the interpolation method used. The raster DTM on the other hand is affected by the cell size used and by the method of interpolation used. Large cell sizes tend to reduce the accuracy while smaller cell sizes have higher accuracies. However, smaller cell sizes tend to slow down the processing due to high memory space needed to create the necessary files and can be very slow when working with large areas.

4.2 Building Modelling

The buildings are extracted from the rectified aerial photographs as polygons. However, they need to be converted into raster models so as to enable their combination with the DTM. To that effect, this section discusses the concepts of conversion from the vector into the raster model and the errors associated with that process.

The conversion of vector building models into raster building models is of great significance. This is due to the loss of accuracy associated with these conversions. Figure 4.2 illustrates the process of conversion together with the possible errors associated with it.

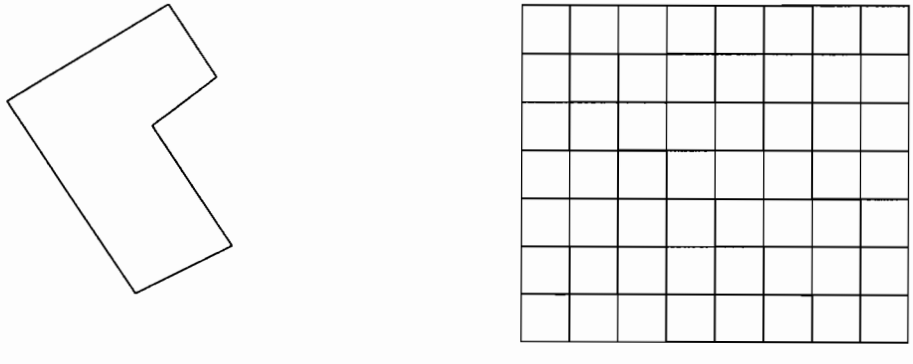

(a) **(b)**

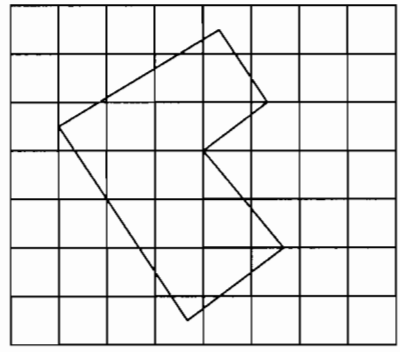

(c)

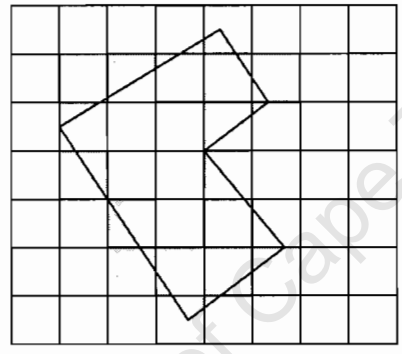

(d)

Figure 4.2: converting vector buildings into raster models

Figure 4.2(a) represents the plannimetric model of a building in vector format produced by digitising the outlines of the building from the aerial photograph. In order to convert the vector building into raster building, the cell size is specified since the conversion transforms the lines into raster cells. Figure 4.2(b) represents the cells which constitute a raster. The cell sizes are limited by the level of accuracy required and also by the availability of computing resources. Figure 4.2(c) depicts a situation where the vector representation is overlaid on the raster surface. The effect of the conversion is shown in figure 4.2(d). Here, the cells which will ultimately be affected are shown by the grey shading. It is thus apparent that the vector to raster conversion process results in loss of accuracy and depending on the purpose of the exercise, the effects can be very negative on the modelling results. To that effect, this section attempts to elaborate further on the likely errors caused by the conversion.

The cell representation found in the raster format causes the edges of the building to shift to the outer edge of the cells. This situation results in positional error, which will in turn cause aerial error and volumetric error.

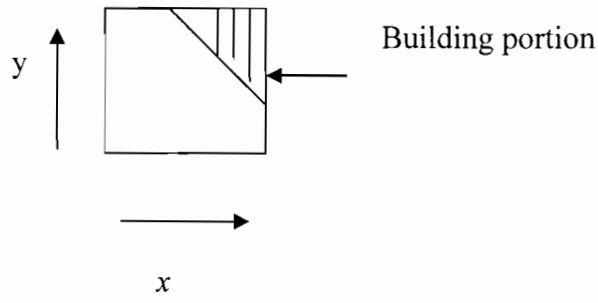

Figure 4.3: plannimetric error

Figure 4.3 shows a portion of building passing through a cell in the x and y arbitrary coordinate system. The portion of a building is shown by the shaded area. In the raster representation, that portion of a building will be represented by the entire cell and there will be errors in the x as well as in the y direction. Both the shape and size of the building are greatly affected by the raster representation as depicted by figure 4.3. The portion of the building passing through the cell is enlarged by the unshaded area. The effect of change of shape is clear in figure 4.2(d). Here the new shape follows the outer edges of the shaded cells.

The maximum error in the plannimetric position is given by the maximum change in x and the maximum change in y. Since the algorithm works in such a way that it searches for a line within a particular cell and it gives the whole cell a value of 1 if it finds the line or 0 if there is no line present, the maximum error possible is approximately equal to the size of the cell. This is because, if only a tip of line is passing through a cell, then the whole cell is given a value of 1. Thus the accuracy heavily depends on the size of the cell. The maximum plannimetric error is the diagonal given by:

$$maximum\ plannimetric\ \ error = \sqrt{(x^2 + y^2)} \qquad 4.1$$

Hence for a cell of size 1m, the maximum plannimetric error is equal to the square root of 2m.

It is important to note that in all cases an overestimation of the building size (aerial and volumetric) results from the vector to raster conversion. This translates into an overestimate of the obstructions caused by buildings and hence a conservative model of view.

4.2.1 Arial error

The maximum aerial error resulting from the raster representation can be estimated by the number of cells representing the line. A simple technique is to measure each line of the building outline and to divide it by the cell size. Multiply the result by the area of a cell and then add up all areas for the lines constituting the building.

Mathematically, if a building has sides of lengths $l_1, l_2, ..., l_n$, and a raster of cell size p, then the maximum aerial error due to rasterisation is given by;

$$max\ e_A = \left[(\sum_{i=1}^{n} (l_i / p)) * p^2 \right] \qquad 4.2$$

However, the cells constituting the corners are counted twice because of the two lines that meet at the corner. Therefore, the area needs to be adjusted for the effects of the corners by making sure that a corner is only counted once. Thus equation 4.1 can be adjusted to take into account the corners as follows:

$$max\ e_A = \left[(\sum_{i=1}^{n} (l_i / p)) * p^2 \right] - np^2 \qquad 4.3$$

where n is the number of corners.

4.2.2 Volumetric error analysis

The error in volume caused by the raster model is given by multiplying the aerial error by the height of the building as represented by equation 4.3. No additional volumetric error is added due to rasterisation, as this only leads to errors in the horizontal dimension.

$$max\ e_V = e_A * h \qquad 4.4$$

4.3 Combining the DTM and the buildings model

After generating the DTM and the buildings model, the next task would be to combine the two models. Since both models are in raster format, their combination is straight forward as it is a simple case of adding together corresponding raster cells. It should be noted that raster cell values of the building model represent the building height for the particular building being analysed. Similarly, the raster cells of the DTM represent the height of the terrain above the mean sea level at that particular location occupied by the cell.

Figure 4.4 illustrates the combination of a building with the terrain:

5	5	6	6	5	4
4	4	6	6	5	4
4	5	6	5	5	5
6	5	6	5	5	4
6	6	6	6	6	5
6	5	4	3	5	4

(a)Raster DTM

0	3	3	3	0	0
0	3	3	3	3	0
0	3	3	3	0	0
0	3	3	3	3	0
0	3	3	3	3	0
0	3	3	3	3	0

(b)Raster building model

5	8	9	9	5	4
4	7	9	9	8	4
4	8	9	8	5	5
6	8	9	8	8	4
6	9	9	9	9	5
6	8	7	6	8	4

(c) Combined model

A raster model of buildings is represented graphically as illustrated by figure 4.4(b). The vector model of the building is represented by the polygon in figure 4.4(b) while its raster representation is represented by cells bound by the polygon in figure 4.4(c). As mentioned previously, the raster representation enlarges the building it represents by a maximum error which is approximately equivalent to the cell size. Note that the cells representing the building have equal height values and those that are outside the building have a value of zero. On the other hand, the cells of the DTM have height values that vary with height of the terrain and are represented by figure 4.4(a). The combination of the two raster cells yields, figure 4.4(c). It is essential to analyse at this point the values of the combined model containing the building. Apparently, the raster model here gives the building with varying heights when in reality the absolute height of a building should be constant. The situation would not be a problem if the terrain was flat which is seldom the case in real life situations. Clearly, the model is not yet representing reality. In real life, the ground is levelled first before the building is erected. This involves cutting and filling – a procedure of moving earth to level the ground.

In order to minimise the error caused by the combination of the two raster models, the cells on the terrain covering the building area are re-sampled by finding the average height of the cells or by calculating the average height of the building in the combined model. The average height would take into account the effect of the uneven terrain thereby simulating cut and fill. The cut and fill effect can take any height depending on the nature of the terrain. This means that the construction company can choose to make the height 6m, 7m, 8m or 9m the final building height within the boundaries of the erf. In this research it is assumed that the amount of cut is equal to the amount of fill, and the average height of the terrain under the building footprint simulates this scenario.

4.4 Viewshed Analysis

The effect of the raster models is different for mountain views and for ocean views. This is because mountain views are inclined upwards whereas ocean views are views in a downwards direction. In this section, the investigation treats ocean views and mountain views separately.

4.4.1 Mountain views

Assuming a scenario as depicted by figure 4.6 where a mountain is behind a building obstructing the view of an observer in another building, the task in this case is to ascertain mathematically the errors in view arising from the rasterised models.

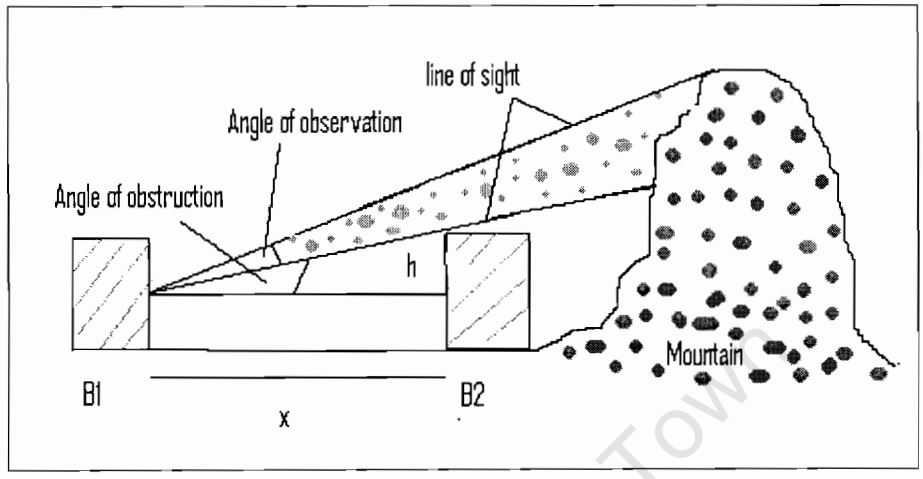

Figure 4.5: Mountain view analysis

Figure 4.5 depicts an observer in a building B1 viewing a mountain. Building B2 is blocking the observer from having a full view of the mountain. In this case both B1 and B2 are assumed to be on level ground. The distance between B1 and B2 is given by *x,* and the height of the obstruction is given by *h* (which is the difference in height between the height of the observer and the height of the obstructing building).

In a rasterised model, the error in the distance between the observer and the obstructing building is affected by the size of the cell. Assuming a cell size of 1m, the maximum error in distance due to rasterisation is approximately equal to the cell diagonal of $\sqrt{2}$ m, hence the distance is equal to (x-$\sqrt{2}$). Here it is assumed that the observer has no positional error.

The following derivation by Whittal (2006) obtains the error in θ for mountain views if θ_1 is the vertical angle to the obstruction, and θ_2 is the same but considers the error due to rasterisation, the error in θ mountain = $\theta_1 - \theta_2$ which equals:

$$e_{\theta\,mountain} = \arctan\left[\frac{h}{x}\right] - \arctan\left[\frac{h}{(x-\sqrt{2})}\right] \qquad 4.5$$

Where $\theta_1 = \frac{h}{x}$ and $\theta_2 = \frac{h}{x-\sqrt{2}}$

Now $\arctan x - \arctan y = \arctan\left[\frac{x-y}{1+xy}\right]$ for x y >-1 4.6

Therefore, from equation 4.6, equation 4.5 can be expanded as follows:

$$\Delta\theta_{mount} = \arctan\left(\frac{h}{x}\right) - \arctan\left(\frac{h}{x-\sqrt{2}}\right) = \arctan\left[\frac{\frac{h}{x} - \frac{h}{(x-\sqrt{2})}}{1+\frac{h^2}{x(x-\sqrt{2})}}\right] \quad 4.7$$

$$= \arctan\left[\frac{\frac{h(x-\sqrt{2})-hx}{x(x-\sqrt{2})}}{\frac{x(x-\sqrt{2})+h^2}{x(x-\sqrt{2})}}\right] \quad 4.8$$

$$= \arctan\left[\frac{h(x-\sqrt{2})-hx}{x(x-\sqrt{2})+h^2}\right] \quad 4.12$$

Equation 4.12 gives the maximum error in view angle to the mountain in the vertical dimension, which can be attributed to errors in plannimetry caused by rasterisation.

Or in general $\Delta\theta_{mount} = \left[\frac{h(x-\sqrt{2}c)-hx}{x(x-\sqrt{2}c)+h^2}\right]$ 4.9

Where c = cell size

h = height of observer with respect to height of the obstacle

x = horizontal distance from the observer to the obstacle

4.4.2 Ocean view analysis

Ocean views are only important to observers on a flat land if there is no obstruction or to observers on a sloping ground. For observers on a sloping ground, it is still possible for them to have clear views of the ocean in the presence of obstruction. In this case the feature being viewed is at the lowest level i.e., mean sea level is zero metres. Therefore, for properties on a flat land with obstruction, the view can be assumed to be zero buildings are situated anywhere within the property boundary according to the zoning regulations of the neighbourhood of that particular property. However, for properties on sloping ground, the view will vary with the height of the ground and the height of the building.

As depicted by figure 4.6, the angle of observation θ for the ocean view is given by

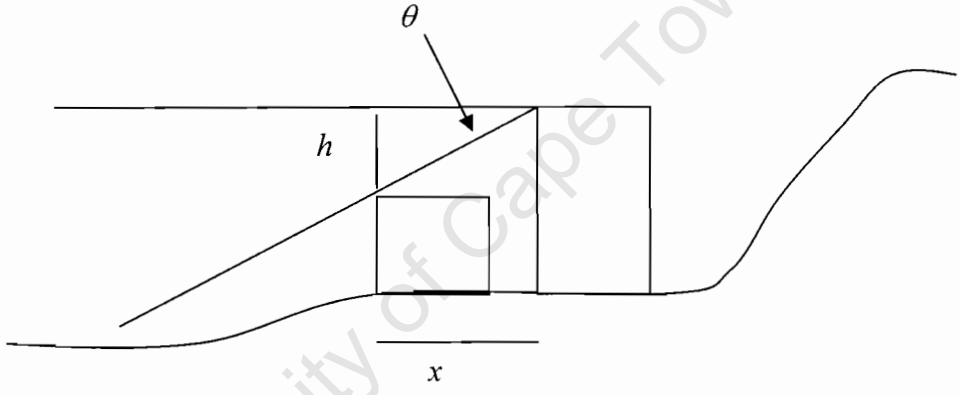

Figure 4.6: Ocean view analysis

$$\tan\theta = h / x \qquad 4.10$$

Where h is the height difference between the observer and the height of the obstructing building, and x is the distance between the observer and the end of the obstructing building. In a raster representation, the end of the building may be extended by the size of the cell.

The following derivation by Whittal (2006) obtains the error in θ for ocean views if θ_1 is the vertical angle to the obstruction, and θ_2 is the same but considers the error due to rasterisation, the error in θ ocean = $\theta_2 - \theta_1$ which equals:

The error in view angle to the ocean due to rasterisation is given by:

$$\Delta\theta_{ocean} = \theta_2 - \theta_1 \qquad 4.11$$

Where $\theta_1 = \frac{h}{x}$ and $\theta_2 = \frac{h}{\sqrt{2}+x}$

$$\Delta\theta_{ocean} = \arctan\left(\frac{h}{x+\sqrt{2}}\right) - \arctan\left(\frac{h}{x}\right) \qquad 4.12$$

From equation 4.6:

$$\Delta\theta_{ocean} = \arctan\left[\frac{\frac{h}{(x+\sqrt{2})} - \frac{h}{x}}{1+\frac{h^2}{x(x+\sqrt{2})}}\right] \qquad 4.13$$

$$= \arctan\left[\frac{\frac{hx - h(x+\sqrt{2})}{x(x+\sqrt{2})}}{\frac{x(x+\sqrt{2})+h^2}{x(x+\sqrt{2})}}\right] \qquad 4.14$$

$$= \arctan\left[\frac{hx - hx - \sqrt{2}h}{x(x+\sqrt{2})+h^2}\right] \qquad 4.15$$

$$= \arctan\left[\frac{-\sqrt{2}h}{x(x+\sqrt{2})+h^2}\right] \qquad 4.16$$

= maximum error in view angle to the ocean, in the vertical dimension which can be attributed to errors in plannimetry caused by rasterisation.

Or in general $\Delta\theta_{ocean} = \arctan\left[\frac{-\sqrt{2}ch}{x(x+\sqrt{2}c)+h^2}\right]$ 4.17

Where c = cell size

h = height of observer with respect to height obstacle

x = horizontal distance form the observer to the obstacle

4.5 Error analysis

Given a nonlinear function:

$$Y = F(a,b,c) \qquad 4.18$$

Given that a, b, and c are independent variables, the special law of error propagation states that the variance of Y which is represented by σ_y^2 is given by the following equation:

$$\sigma_y^2 = (dF/da)^2 * \sigma_a^2 + (dF/db)^2 * \sigma_b^2 + (dF/dc)^2 * \sigma_c^2 \qquad 4.19$$

Considering the case of a simple triangle:

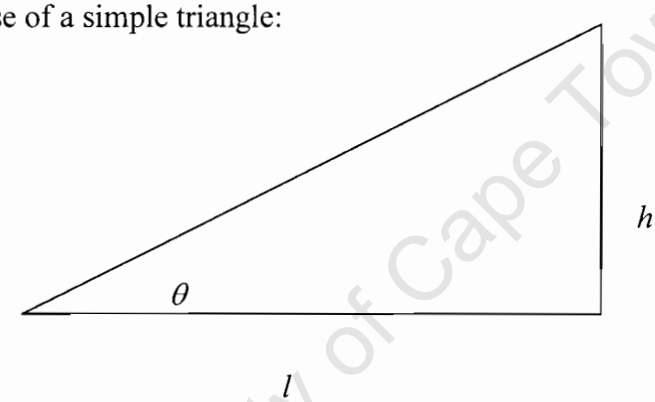

Given that the length of the triangle l is observed as well as the height h. The angle θ is related to h and l as follows:

$$\tan\theta = h/l = F(\theta) \qquad 4.20$$

Given that h and l are independent variables and that the variances of h and l are σ_h^2 and σ_l^2 respectively, the error in θ can be derived from the general law of error propagation by taking partial derivatives as follows:

$$\left[\frac{dF(\theta)}{d\theta}\right]^2 .\sigma_\theta^2 = \left[\frac{dF(\theta)}{dh}\right]^2 .\sigma_h^2 + \left[\frac{dF(\theta)}{dl}\right]^2 .\sigma_l^2 \qquad 4.21$$

4.25 reduces to equation 4.26

$$\sec^4\theta.\sigma_\theta^{\,2} = \frac{1}{l^2}.\sigma_h^{\,2} + \frac{h^2}{l^4}.\sigma_l^{\,2} \qquad 4.22$$

Therefore the error in θ is given by equation 4.23:

$$\sigma_\theta = \sqrt{\frac{\left(\frac{1}{l^2}.\sigma_h^{\,2} + \frac{h^2}{l^4}.\sigma_l^{\,2}\right)}{\sec^4\theta}} \qquad 4.23$$

Given an observer at variable distances from the obstructing buildings as well as the error in distance due to rasterisation and errors in height of the building, table 4.1 gives the worked errors in θ. For an area with a contour interval of 5m, with the closest distance between contours equal to 5m and the furthest distance equal to 10m, the gradient for the closest distance is 1, and the gradient for the 10m distance is 0.5. By assuming that the gradients are equal to the maximum error in height, the maximum error in height is assumed to take values of 1m and 0.5m respectively and the error in distance due to rasterisation is $\sqrt{2}$. From the above information, different lengths and heights are considered in this worked example to illustrate the effect of the errors in length and height on the angle θ. 10m, 15m and 20m are the lengths considered in this illustration. For a medium density suburb, the distance between adjacent properties is about 10m, while that of a house across the road is between 15 and 20m.

Table 4.1: Analysis of the maximum expected standard deviation of vertical observation angle for raster cells of 1m x 1m.

Length (l)m	Height (h)m	θ^0	σ_h (m)	σ_l (m)	σ_θ (^{0})
10	1.5	8.53	0.5	$\sqrt{2}$	0.15
15	1.5	5.71	0.5	$\sqrt{2}$	0.06
20	1.5	4.29	0.5	$\sqrt{2}$	0.04
10	4.5	24.23	1.0	$\sqrt{2}$	0.51
15	4.5	16.70	1.0	$\sqrt{2}$	0.24
20	4.5	12.68	1.0	$\sqrt{2}$	0.14

Table 4.1 shows the calculated errors in observation angles using equation 4.27. From table 4.1 it can be concluded that the error in observation angle increases as the distance between the observer and

the surrounding buildings posing as obstruction gets smaller. The error also increases with increased height of the building. Therefore, a large error in observation angle is expected from a large error in DTM. However, due to the position of the observer with respect to the obstructions, it is not possible to ascertain the effect of this error on view.

CHAPTER FIVE: EXPERIMENTAL METHOD

This chapter outlines the experimental method developed in this research work. The first task was to select a study area for the experimentation. The study area needed to comply with the International Association of Assessing Officers (IAAO) requirements in terms of number of sales. With respect to this research work, the area needed to be close to the ocean and to the mountains so as to enable the analysis of the respective views. GIS software and CAMA software were also chosen for use during the model development and during the analysis stage. The ESRI ArcGIS 9 product was used for the development of the GIS while the NCSS package was used for the CAMA analysis. ArcGIS 9 has capabilities to handle data in three dimensions and it allows one to perform terrain modelling using 3D Analyst extension. The software also enables map generation quickly and can be customised to facilitate application development. NCSS is a statistical software used to build the CAMA models. This is made possible by its ability to handle several variables and to perform regression analysis. Within NCSS, one is allowed to enter the model and the transformations that are done on several variables. The major strength of NCSS among others is its ability to import data from various sources, i.e., it is compatible with other data management software programs.

5.1 Study area

The Sea Point suburb falls within the Quartile 4 modelling region in terms of CAMA modelling used by the City of Cape Town during the GV2000 Valuation Project. It was chosen as the study area because it is located between the mountains and the ocean, which form two important views in the City. The gradient in this area varies leading to properties on a relatively flat area, and some on sloping ground.

The property type within this area is a mixture of single-storey residential and multi-storey residential as well as commercial properties. An important aspect required by the IAAO is that the neighbourhood should have a minimum of 100 sales within a particular period so that it qualifies for CAMA analysis. Analysis of the sales data for the period January 1998 to July 2000 revealed that the Sea Point area had sales of more than 100. The sales were cleaned first by eliminating non-market sales. This was done by dividing the sale price by the Total Living

Area. In this case, outliers were marked with a 3 which implied that such sales were non-usable and the good ones were marked with a 1. The results are shown in Appendix C.

5.2 DTM and buildings model generation

The Lo19/WGS84 spatial reference system was used in this research. The height data source for the DTM was 1: 50 000 topographic mapping with contour lines, while an aerial photograph of scale 1:10 000 was used as the source of data for the buildings model. The following stages were followed during the generation of the DTM and the buildings model:

- Georeferencing of the map and digitisation of contours
- Interpolation of the surface from the contours
- Generation of buildings model from the aerial photograph
- Combining of the DTM and the buildings model

5.2.1 Map Georeferencing and contour digitisation

The 1: 50 000 map sheet was first scanned and saved as a jpeg image. The image was then imported into ArcGIS 9 for georeferencing. During the georeferencing process, four points whose real world coordinates were known were identified on the map and these were used to generate the transformation parameters which were then used to transform the digital map local coordinates to the real world coordinates. Although the affine transformation was used, it is embedded in the GIS system and is not available to the user. However, a precision output is given at the end of the procedure.

Contour digitisation

The contours were then digitised using the on-screen digitising method. The contours on the map were given at a height interval of 5m. The heights of the contours were entered into the table of attributes manually after digitising of every contour line. The snapping tolerance of zero mm was set.

5.2.2 Interpolation of the terrain surface from the contours

Delaunay triangulation was used to generate the TIN surface. The algorithms used are embedded within the GIS system. The grid DTM was also produced from the contours. A grid

size of 1m was chosen because it takes less memory space and hence faster to work with than smaller grid sizes.

TIN generation

The sequential steepest slope method was used to interpolate the TIN. The following procedure in ArcGIS is followed:

- Open 3D Analyst
- Click create TIN from features
- Specify the contours as the features

Grid DTM generation

- Open the 3D Analyst
- Click on generate grid from features
- Specify the TIN as the source
- Specify the grid size
- Specify the nearest neighbour as the method of interpolation
- Click ok

The accuracy of the TIN model and of the raster DTM were assessed by comparing the heights of the town survey marks (TSM's) identified in the study area and the actual heights on the models. A standard error in height was then produced for each model.

5.2.3 Generation of buildings model

An aerial photograph of the area under study was used as the source of the buildings. This was because it was not possible to get the building plans from the responsible authorities due to security reasons. The aerial photograph was rectified first to remove distortions due to relief and tilt of the plane. The photograph was then imported and georeferenced in ArcGIS 9. The building outlines were then digitised on the aerial photo and the information about their heights was stored in the attribute table. All single-storey buildings were assumed to have a height of 3m. This is the standard height according to the building regulations of the City of Cape Town.

Vector to raster conversion

The vector model of the buildings was then converted to the raster model. The conversion of the vector buildings into raster proved to be a real challenge as there was no straight procedure one could use for the conversion. The aim was to ensure that a surface covering the entire area was converted into raster. To that effect, a boundary was generated around the entire area of investigation and this was assumed as a building within the system with zero height. This ensured that all areas with no buildings would get a value of zero otherwise they would get a "no value" code which would complicate the combination of the buildings and the DTM. A raster cell size of 1m was used.

5.2.4 Combining the DTM and the building models

After ensuring that both the DTM and the buildings model were in the same grid format, they were then combined together into one surface. Since the surfaces were made of grids, corresponding grids were added up together. The resultant surface was a model of the terrain and the buildings. The following procedure is followed in ArcMap:

- Open the ArcTool Box
- Click on raster maths
- Click on addition
- Specify the grid DTM and the raster buildings

Using raster algebra [Combined surface] = [Input DTM] + [Building model]

5.3 Viewshed Analysis

Two observers were simulated for every building that was analysed for viewshed. One observer was positioned in front of the side facing the ocean and the other one was positioned in front of the side facing the mountain. Only ground floor observers were simulated in this research. Viewshed analysis was then performed for all the observers to determine the quantity of view. The number of visible cells on each viewshed map was exported into excel for further processing in CAMA.

5.4 Exporting of the results into NCSS for CAMA analysis

The processed viewshed results were then exported into NCSS for the CAMA evaluation analysis. The view values were identified by their property identifiers which enabled them to be linked with the property data in NCSS. The model used during the GV2000 for the Quartile 4 region was adopted. Since the results will be tested against the results during GV2000, the same model used for GV2000 was used in this study. A new field with the new view factors was created and the model was run with the new view values. The model shown in equation 5.1 was used to run the new view values.

SP =MOS^(0.3504352)*TSTRSAVAR^(0.5955746)*RSAHiVar^(0.4085364)***view_linked***
Q4SUBLV21^(1.003756)*Q4TRAFLV^(1)*MicroNBLin^(1)*((Q4QUALLV^(1)
*Q4CONDLV^(1)*SizeAdj^(0.291578)*STOREYLV^(0.9888958)*(1.177319)^GRPHSG*
((18472.51)*TOTFIX3+(1959.165)*TotLivArea))+((364.0818)
*RATEABLE_EXT)+((500)*GarCp +(400) *D_POOL)) **5.1**

Where SP is the sale price of the real property, MOS represents the Month Of Sale adjustment, TSTRSAVAR, RSAHiVar, and Q4SUBLV are location adjustments, Q4TRAFLV represents the traffic factor adjustment, MicroNBLin is a micro-neighbourhood factor, Q4QUALLV is the quality of the building, Q4CONDLV is the condition of the building, SizeAdj is a factor that takes into account the size of the living area, STOREYLV is the storey level adjustment, and view linked refers to the view factor.

The data is imported into NCSS from the database. The variables shown in equation 5.1 are stored in the variable window. The relationships between the variables as shown in equation 5.1 are specified in the transformation window. The model is then specified in the regression analysis window and is processed.

The model given by equation 5.1 was developed for the entire Quartile 4 modelling region and in this research it is used to test only properties in Sea Point. The major disadvantage of

this approach is that the model may not be as good a representation of the Sea Point property values as it is of the entire Quartile 4 property values.

5.7 Ratio analysis

The ratio studies explained in chapter four were used to analyse the accuracy of the results estimated by the model with new view factors. The results were compared with those achieved with the old view factors used in the GV2000 Project as well as with those recommended by the IAAO organisation as explained in Chapter Three.

5.8 Market Value comparisons

The market values estimated using the new view values computed from the view modelling were compared with the market values produced during the GV2000.

CHAPTER SIX: RESULTS AND ANALYSIS

The purpose of this chapter is to present the results of this research and to report on the analysis performed on the results. The chapter begins by explaining the geographical characteristics of the study area. The geography of the study area is very crucial to this study because the determination of view is based on GIS and 2.5D modelling. The generation of the DTM is explained in the following section. In this regard, the results of the TIN and raster DTM are presented. The modelling of buildings follows the DTM modelling, after which the DTM and the buildings are combined. The results of view analysis are also given as well as the application of the results in the CAMA model.

6.1 Case study area analysis

In this section, the study area is explored by means of exploring the property inventory data used to run the CAMA models as well as the geographical characteristics of the area.

Figure 6.1: Geographical characteristics of the study area

As depicted by figure 6.1, the Sea Point suburb is located between the ocean and the mountain. Along the seaboard, the property type is Sectional Title flats and as one moves away from the ocean towards the mountain, one finds single residential properties.

6.2 Digital Terrain Modelling (DTM)

This section presents the results of the digital terrain modelling. The results of the TIN model and the raster model are explained.

6.2.1 Contour digitisation

The contour map was scanned at the resolution of 400 dots per inch. This resolution was high enough to enable high accuracy digitisation of the contours. Before, the digitisation process, the scanned images were exported into ArcGIS for georeferencing. The image was georeferenced by clicking on a known point and entering the real world coordinates into the table provided. At the end of the process, an accuracy reported was generated which gives the accuracy of digitisation. The root mean square error for georeferencing was 0.004mm. For a map of 1:50 000, it means that the error on the ground is 20cm.

6.3 Contour data

The contours were digitised and added to ArcScene, an Arc GIS module, for visualisation.

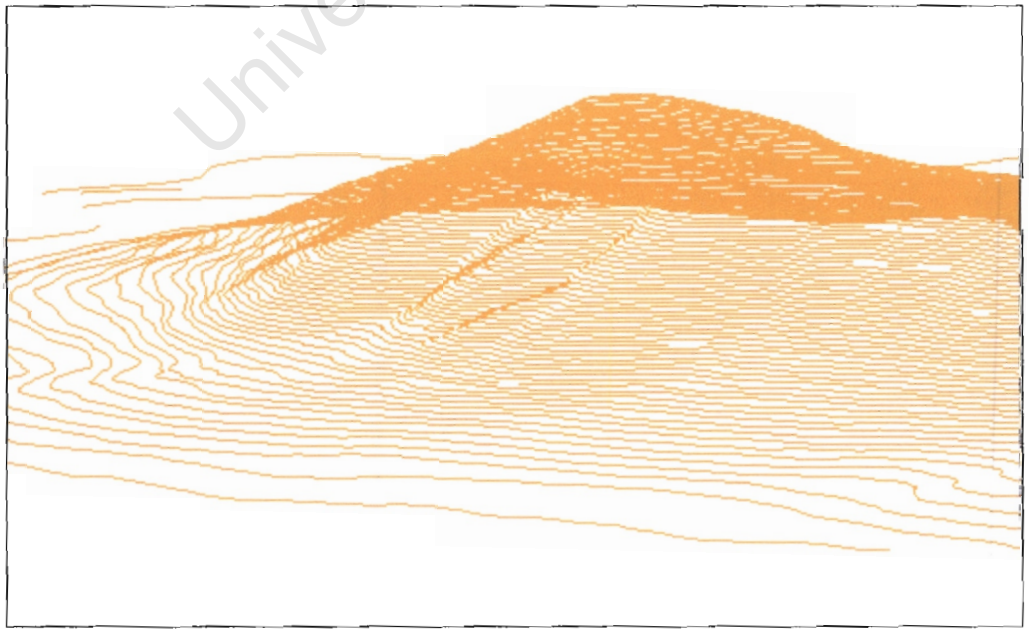

Figure 6.2: Perspective view of the contour data

Figure 6.2 shows that perspective 3D contours of a surface can be used for visualisation purposes (Naser et al, 2005). From the figure, the mountain peak as well as the mountain foot, which in this case represents the shoreline, are quite distinct.

6.4 TIN model

The TIN model was generated from the contours shown in figure 6.2. The edge-based data structure was used because it utilises Delaunay triangulation. Recalling from chapter three, the method of Delaunay triangulation is the best at generating triangular surfaces because it ensures that best geometry is achieved for every triangular surface.

Figure 6.3: TIN model

The resulting TIN model is depicted in figure 6.3. The TIN model represents a continuous surface as opposed to the contour model which is discontinuous between the contours. The main advantage of the TIN model is its ability to model the terrain characteristics more efficiently. Chen and Tobler, (1986) point out that peaks and pits are modelled very well using the TIN method, hence its usefulness for visualisation analysis. As shown in figure 6.3, the mountain peak and the small streams/gullies that run down the mountain are quite visible.

Further analysis can be performed on the TIN model by overlaying the aerial photograph over the TIN, called draping. A facility is provided in ArcScene that makes it possible to drape the aerial photo on top so as to perform informed visual analysis.

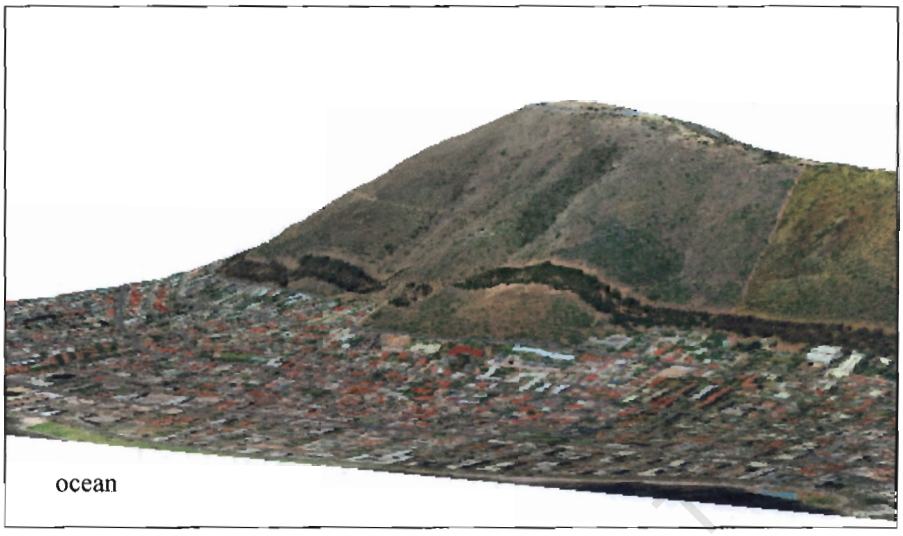

Figure 6.4: Aerial photo draped on TIN

As clearly depicted by figure 6.4, the draped photograph gives a more realistic visual impression of the terrain. The location of the buildings relative to the mountain and the ocean can be clearly visualised, although a closer inspection will reveal that the buildings have no 3rd dimension, and are simply footprints on the TIN.

A draped photograph provides a visual check of the gross accuracy of the DTM. This technique however, requires that the analyst be familiar with the area being modelled so that he/she will be able to assess whether the features on the aerial photograph are mapping well to their corresponding features on the TIN model. In this case, the mountain peak on the DTM is coinciding with the peak on the aerial photo and the ocean is also mapped well. In this way, blunders and gross errors are checked.

Random errors are, however, difficult to assess for DTM's. This is usually because one needs to have a DTM of the same area produced using more accurate methods. In this case a DTM produced from photogrammetric methods or LIDAR methods would have been appropriate to assess the accuracy of the DTM produced here, however, this data was not available.

In order to get an idea of the general accuracy of the DTM, town survey marks (TSM) identified in the Sea Point area were used to assess the DTM accuracy. The TSMs were displayed on top of the TIN model as points using their coordinates. The area directly below the TSM on the TIN was clicked on to get the corresponding height of the DTM. Table 6.1 shows a file of TSMs and their corresponding heights on the TIN as well as their coordinates.

Table 6.1: DTM accuracy table

X(Lo 19/84)	Y (Lo19/84)	Htsm (m)	H_TIN (m)	Difference (d) (m)
-56322.73	-3753856.76	5.182	4.95	0.232
-56493.21	-3754016.98	5.062	4.6	0.462
-56593.53	-3754224.98	5.424	4.83	0.594
-56697.48	-3754423.97	5.89	5.88	0.01
-56697.48	-3754784.96	10.04	9.85	0.19
-56218.1	-3754633.14	29.95	30.08	-0.13
-56130.69	-3754502.53	29.07	29.82	-0.75
-56020.65	-3754341.64	30.09	30.25	-0.16
-55977.54	-3754599.73	65.11	65.32	-0.21
-56031.1	-3754691.46	64.93	64.81	0.12
-56093.74	-3754786.91	60.21	60.28	-0.07
-56115.77	-3754860.02	60.04	60.23	-0.19
-56166.15	-3754937.61	54.92	54.92	0

$\sum d = 0.098\,\text{m}, \qquad \bar{d} = 0.0075\,\text{m}$

A statistical test was conducted to see if there was significant difference between the mean of the TSM's height and the mean of the TIN using the sampled points.

Calculation of the Standard Error of the Differences:

$$\text{SSD} = \sum_{i=1}^{10} d_i^{\,2} - \left(\sum d_i\right)^2 / 13$$

SSD= 1.360804-(0.0096/13)

SSD = 1.36m

$$s_{\bar{d}} = \sqrt{\frac{SSD}{13(13-1)}}$$

$$= \sqrt{0.0087}$$

$$s_{\bar{d}} = 0.093\text{m}$$

Testing the significance of the differences in mean between the TSM and the DTM using the Two-tailed t-test:

$$t = \frac{\bar{d}}{s_{\bar{d}}} = \frac{0.0075}{0.093} = 0.081$$

$$H_0 : \mu_{TSM} = \mu_{DTM}$$

$$t_{.05}(12d.f) = 2.179$$

The calculated value of t is smaller than the critical value at the 95% level; therefore, $\mu_{TSM} = \mu_{DTM}$, or there is no significant difference in the two means.

6.5 Raster DTM

The raster DTM with a cell size of 1m by 1m was generated from the contours using the sequential steepest slope algorithm explained in chapter three.

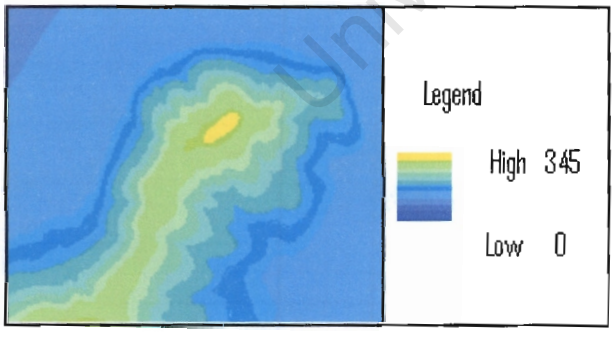

Figure 6.5 Raster DTM

Figure 6.5 shows the raster model with variations in colour representing variations in height. The yellow band which lies on the diagonal represents the mountain top. It is however difficult to conduct visualisation analysis on a raster DTM. Therefore, its applications are mainly limited to mathematical modelling. The discontinuity property of the raster DTM is

quite apparent on the image mainly where there is a change in colour. However, the discontinuity can be reduced by reducing the cell size.

The accuracy of the raster model was also assessed using the TSM's and the results are shown in table 6.2.

Table 6.2 Raster DTM accuracy table

X (Lo19/84)	**Y**(Lo19/84)	**Htsm (m)**	**Hraster (m)**	**Difference(d) (m)**
-56322.7	-3753857	5.182	4.95	0.232
-56493.2	-3754017	5.062	4.6	0.462
-56593.5	-3754225	5.424	5.63	-0.206
-56697.5	-3754424	5.89	5.88	0.01
-56697.5	-3754785	10.04	9.85	0.19
-56218.1	-3754633	29.95	30.08	-0.13
-56130.7	-3754503	29.07	30.43	-1.36
-56020.7	-3754342	30.09	30.25	-0.16
-55977.5	-3754600	65.11	65.32	-0.21
-56031.1	-3754691	64.93	64.81	0.12
-56093.7	-3754787	60.21	60.78	-0.57
-56115.8	-3754860	60.04	60.23	-0.19
-56166.2	-3754938	54.92	55.36	-0.44

Calculation of the Standard Error of the Differences:

$\bar{d} = -0.173\,\text{m}, \qquad \sum = -2.252\,\text{m}$

$$\text{SSD} = \sum_{i=1}^{13} d_i^{\,2} - \left(\sum d_i\right)^2 / 13$$

SSD= 2.851-(5.072/13)

SSD = 2.4609

$$s_d = \sqrt{\frac{SSD}{13(13-1)}}$$

$$= \sqrt{0.015775}$$

$$= 0.13\text{m}$$

Testing the significance of the differences in mean between the TSM and the raster DTM using the Two-tailed t-test:

$$t = \frac{\bar{d}}{s_{\bar{d}}} = \frac{-0.173}{0.13} = -1.33$$

$$H_0 : \mu_{TSM} = \mu_{DTM}$$

$$t_{.05}(12d.f) = 2.179$$

The calculated value of t is smaller than the critical value at the 95% level; therefore, $\mu_{TSM} = \mu_{DTM}$, or there is no significant difference in the two means. Comparing the TIN and the raster DTM, one can notice that the standard error for the raster DTM is larger than that of the TIN. This means that the TIN is modelling the surface more accurately than the raster DTM. Although the raster DTM has a larger error than the TIN, the t-test has shown that there is no significant difference in the mean of the TSMs and raster DTM.

6.6 Building modelling

Buildings were modelled from the aerial photos by capturing polygon data of the footprints on the aerial photo. The property identity (PID) was used to link the footprints to the inventory database maintained by the City of Cape Town. The number of storeys in the database was used as a basis for calculating the height of each building. According to the zoning regulations of Cape Town, a single-storey building is between 3 and 3.3m high. A height of 3m per storey was used in this case and the height of the buildings was determined by multiplying the number of storeys with the height of one storey.

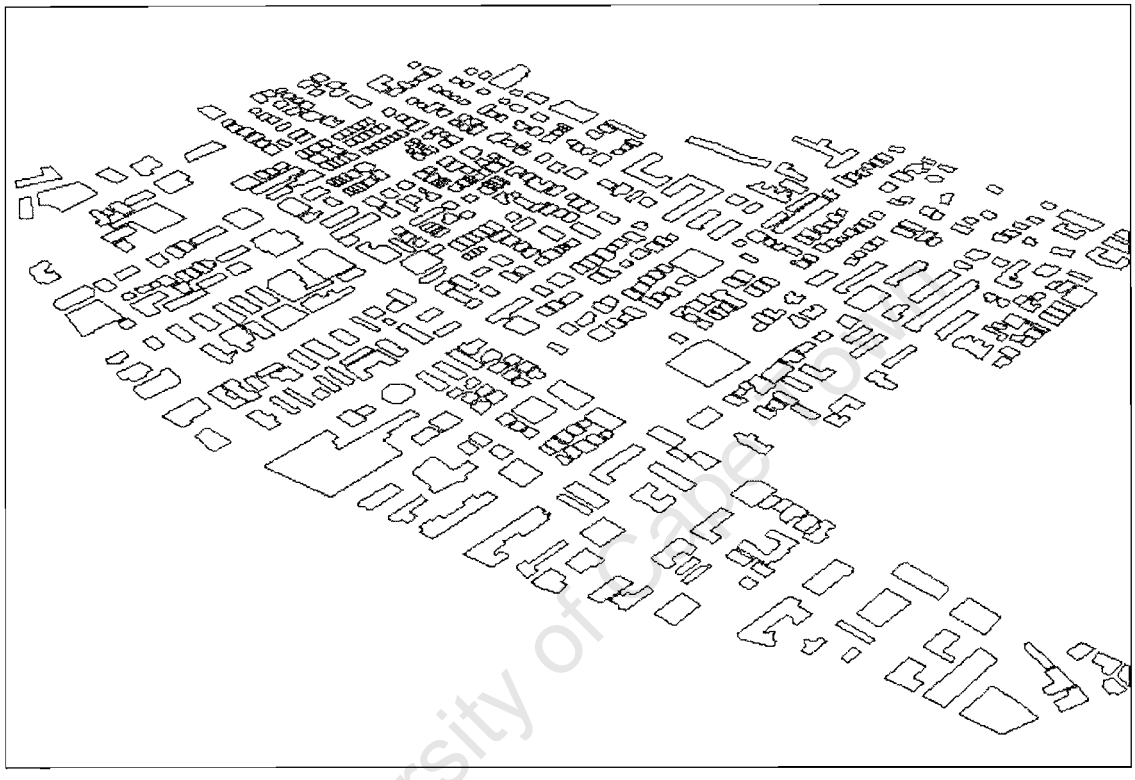

Figure 6.6: Building footprints

Figure 6.6 shows the building footprints generated from the digitisation of buildings on the aerial photograph. A table of attributes containing the building height and the property ID was generated and is shown in appendix B.

A ground survey method using total stations was proposed to assess the accuracy of the building model by surveying a number of buildings and then comparing the surveyed building coordinates with the GIS coordinates of the building model. The surveying technique proved difficult due to the inaccessibility of the houses because of dura-walls and also because of the absence of the owners during the time of survey.

The building footprints were checked for consistency by overlaying them on top of erf boundaries. The footprints must be fully contained within the erven. This kind of check is

useful to guard against outliers. In so doing, it was ensured that no building was protruding onto the road. A script was run to select all the footprints that were not fully contained within the erven. The identified building footprints were recaptured and adjusted. However, this method does not provide an absolute check on the accuracy in position of the buildings on the model.

The building footprints were extruded by their heights and the results are shown in figure 6.7. The extruded buildings were overlaid on top of the aerial photograph. The overlay gives a vivid visual impression of the model.

Figure 6.7: Extruded buildings on the aerial photograph

From figure 6.7 it is clear that beach properties are mainly high-rising flats and commercial properties. As one moves away from the ocean towards the mountain, one finds the single storey residential properties. One important failure of this method of modelling the buildings is that a flat roof is assumed for all properties. This would result in an overestimate of view as the full extent of obstruction of the building is not modelled.

Another way of visualising the model is to overlay the extruded building models on top of the TIN. A more realistic model is achieved and the height relationship between the buildings and the terrain can also be perceived as shown in figure 6.8. One can already see that the buildings along the shore are mainly high-rise and have a great potential for obstructing ocean views for properties further away from the ocean.

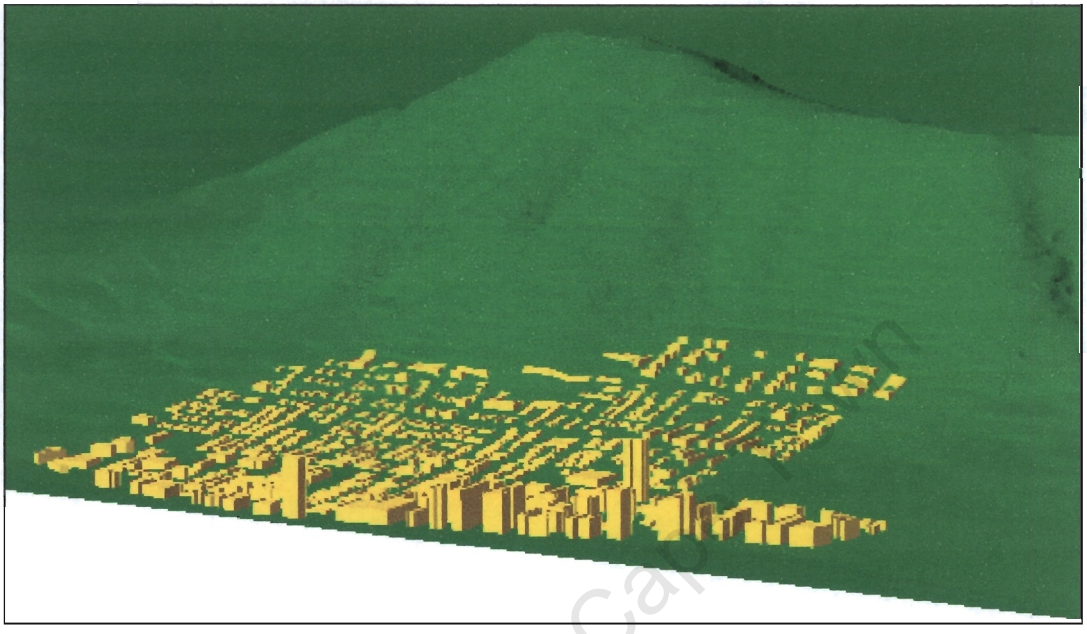

Figure 6.8: Buildings overlaid on the TIN

As depicted in figure 6.8, overlaying the building models onto the TIN presents a problem in that the overlaid building models are twisted in areas where the terrain is not even. This is especially visible on steep slopes towards the mountain. The end result is such that the model gets highly inaccurate in those areas. As a result, the TIN model could not be used for the analysis of view. The other problem was that the building model and the TIN model could not be added together to form one feature.

6.7 Raster building model

As explained in chapter four, the buildings and the DTM can only be combined in the raster format. To that end, a cell size of 1m was used to convert the buildings footprints into a raster model. A dummy building with zero height was created for the areas without buildings. This was to make sure that the entire terrain was covered with buildings. This would then make the

combination of the raster DTM and the raster buildings possible. The same cell size ensured the combination would be a 1 to 1 mapping.

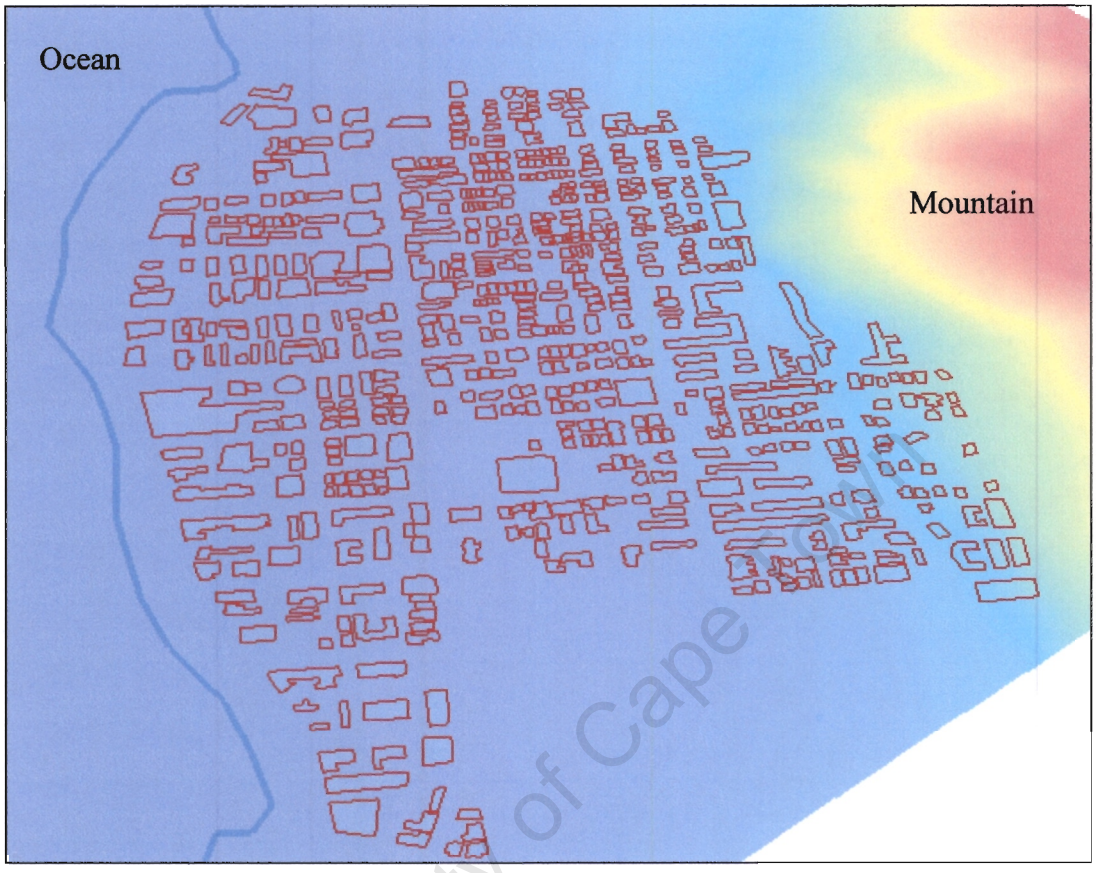

Figure 6.9: Combined model of buildings and raster DTM

Unlike the vector buildings and the TIN model, the raster DTM and the raster buildings combine into one model easily. High height values are obtained where there are buildings and low values for adjacent cells with no buildings. As depicted by figure 6.9, the ocean and the mountain are clearly identified for view analysis.

The accuracy of the buildings on the combined surface was assessed by overlaying the vector buildings polygons shown in figure 6.6 on top of the combined surface as shown in figure 6.10.

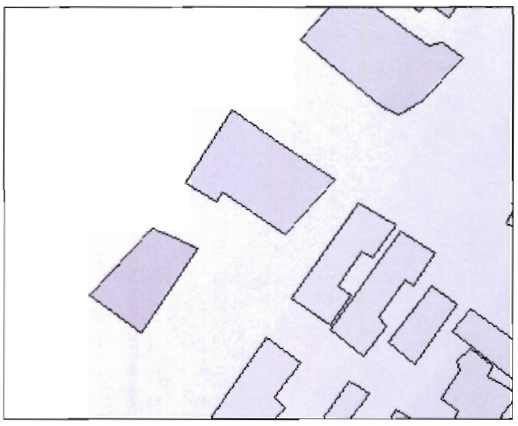

Figure 6.10: Accuracy check for the combined surface

In figure 6.10 the building footprints are overlaid on top of the combined surface. It can be seen that the edges are not smooth due to rasterisation – in some cases a straight building line will appear stepped, and a ninety degree building angle will be greater or lesser. In chapter four, during the conceptual development of the view model, it was ascertained that the maximum error in position due to rasterisation is $\sqrt{2}$ m for a raster cell size of 1m by 1m. In this research however, areas without buildings were made up of polygons which were recorded as buildings with a height of zero. These polygons shared the same boundary lines with the buildings.

After the buildings and the DTM were combined, the surface was now a representation of the real world and could be used for view analysis.

6.8 Viewshed analysis

Observers were simulated on the combined surface. For every building, two observers were simulated, one on the side facing the ocean and another on the side facing the mountain. This was to ensure that both mountain and ocean views were captured. The viewshed analysis in Arc View was performed for all the properties and a table of the results showing the number of cells visible for the mountain and the ocean views is shown in Appendix D.

Viewshed maps with the highest number of visible cells for both the ocean and mountain views were selected. For the ocean views, the beach properties had the highest number of visible cells.

Table 6.3: Best views

Property No.	Visible cells
1	240660
2	200554
3	189993
4	213432
5	198765
6	245980
7	220566
8	237213
9	185332
10	191543
Total	**2124038**
Mean	**212403.8**

Table 6.3 shows 10 beach properties and their corresponding number of visible cells. The average number of visible cells was calculated and this number was assumed to represent the best view.

A *view index* was generated by dividing the total number of visible cells for every observation by the average number given in table 6.3. Table 6.4 shows part of the table with visible counts. The views have been categorised as Ocean view for those with observed ocean views, mountain view, for observed mountain and other for views which are neither ocean nor mountain. The view index is given by the following relationship:

View index = total number of visible cells/212403.8 6.1

Table 6.4: View Index

PID	X(Lo19/84)	Y(Lo19/84)	Ocean	Mountain	Other	View Index
CCT0000098	-56252	-3755016			34231	0.16
CCT0000104	-56529	-3755036		23415		0.11
CCT0000129	-55872	-3753959			33896	0.16
CCT0000132	-55684	-3753995		74321		0.35
CCT0000142	-55974	-3754015			73421	0.35
CCT0000144	-55901	-3754023			46983	0.22
CCT0000144	-55901	-3754023		72314		0.34
CCT0000152	-55980	-3754068		101234		0.48
CCT0000155	-56011	-3754079			85644	0.40
CCT0000159	-56052	-3754089			42461	0.20
CCT0000161	-55991	-3754093			67462	0.32
CCT0000162	-55707	-3754104	164532	44987		0.99
CCT0000165	-56060	-3754112			64326	0.30
CCT0000169	-55678	-3754129		84563		0.40
CCT0000170	-55899	-3754127			53876	0.25
CCT0000171	-55689	-3754138		75648		0.36
CCT0000173	-55913	-3754151		89607		0.42
CCT0000175	-55801	-3754178	133245	22364		0.73
CCT0000177	-55973	-3754173		34568		0.16
CCT0000178	-56023	-3754179			75834	0.36
CCT0000180	-56008	-3754187			44890	0.21
CCT0000184	-55909	-3754204		33546		0.16
CCT0000187	-56044	-3754215		54372		0.26
CCT0000193	-56002	-3754245		67543		0.32
CCT0000195	-56028	-3754269		49854		0.23
CCT0000199	-56537	-3754285			34532	0.16
CCT0000200	-55940	-3754333	132896	43456		0.83
CCT0000202	-56266	-3754347			32896	0.15
CCT0000206	-56289	-3754377			48562	0.23
CCT0000208	-55913	-3754385	98753	78654		0.84
CCT0000212	-56240	-3754409			87465	0.41
CCT0000213	-56096	-3754421	105321			0.50
CCT0000223	-56618	-3754507			46891	0.22
CCT0000225	-56002	-3754543	134576	32456		0.79
CCT0000226	-56199	-3754547		45736		0.22
CCT0000227	-56012	-3754557		43275		0.20
CCT0000229	-56058	-3754560		87564		0.41
CCT0000230	-56017	-3754565	124573	43234		0.79
CCT0000234	-56123	-3754582		85432		0.40
CCT0000238	-56384	-3754687		98453		0.46
CCT0000240	-56363	-3754702	202345	32123		1.00
CCT0000241	-55958	-3754713	112358	66754		0.84
CCT0000247	-56037	-3754733	105439	55687		0.76
CCT0000249	-56037	-3754760	104342	33245		0.65
CCT0000251	-56069	-3754787	87564	33245		0.57
CCT0000259	-56215	-3754829	104986			0.49
CCT0000260	-55991	-3754834	102999	89675		0.91
CCT0000261	-56209	-3754833			64879	0.31
CCT0000261	-56209	-3754833		65432		0.31
CCT0000263	-56264	-3754834			43768	0.21

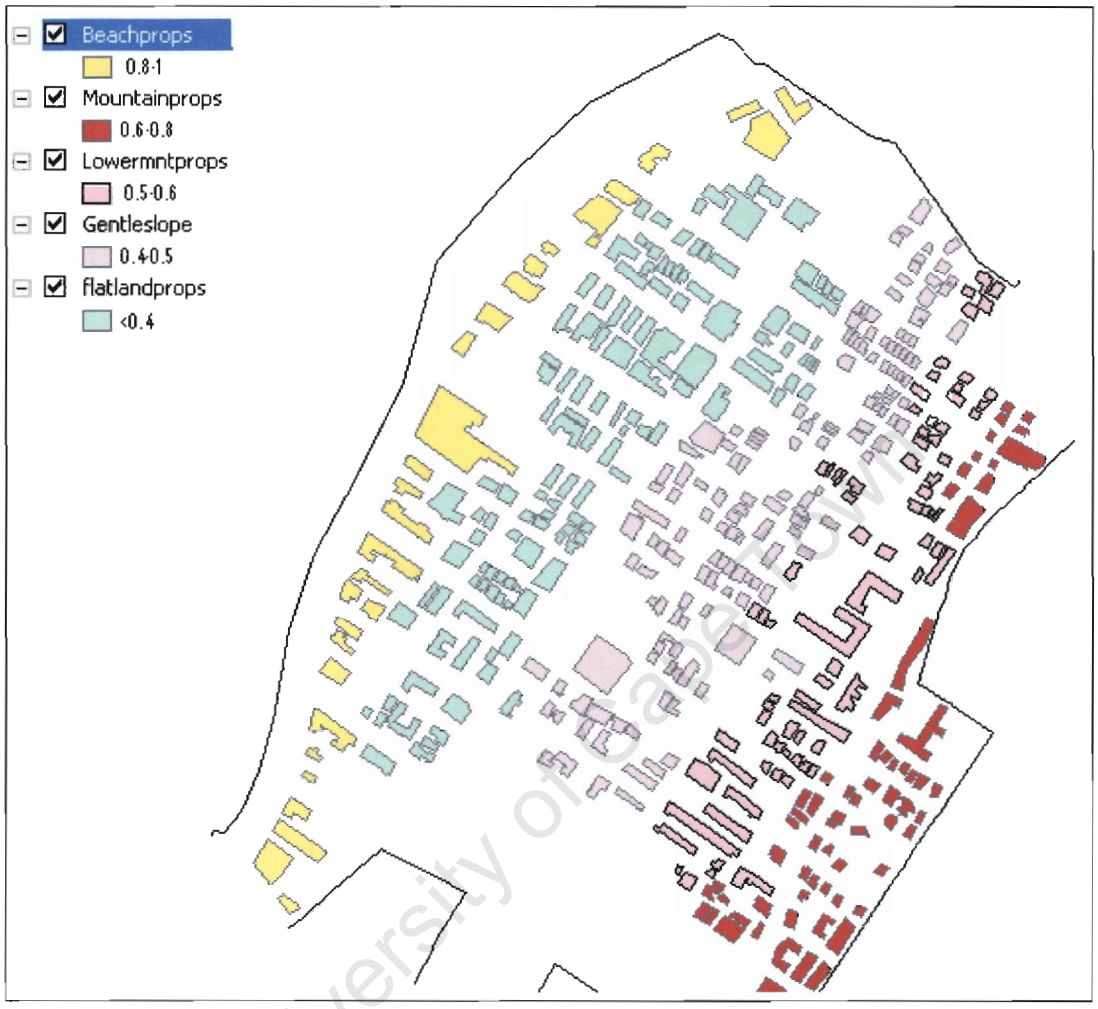

Figure 6.11: View correlated with slope of ground

Figure 6.11 is a map of the results of the view factors for each building. The view factors are classified on a scale as shown in figure 6.11. From the figure, it is clear that the beach properties have the best views which are between 0.8 and 1. Properties on the mountain have the second best views. This is because they are at high elevations thus, obstruction is less. However, the properties close to the mountain have worse views of the mountain itself than those further away due to their height and proximity to the mountain slope. As one moves down hill, the view is reduced due to the relative height of building obstructions to the observer. Properties directly behind the beach properties have the poorest views. This is because they are situated on a relatively flat ground and thus the effect of the obstructions both to the mountain and the ocean is large.

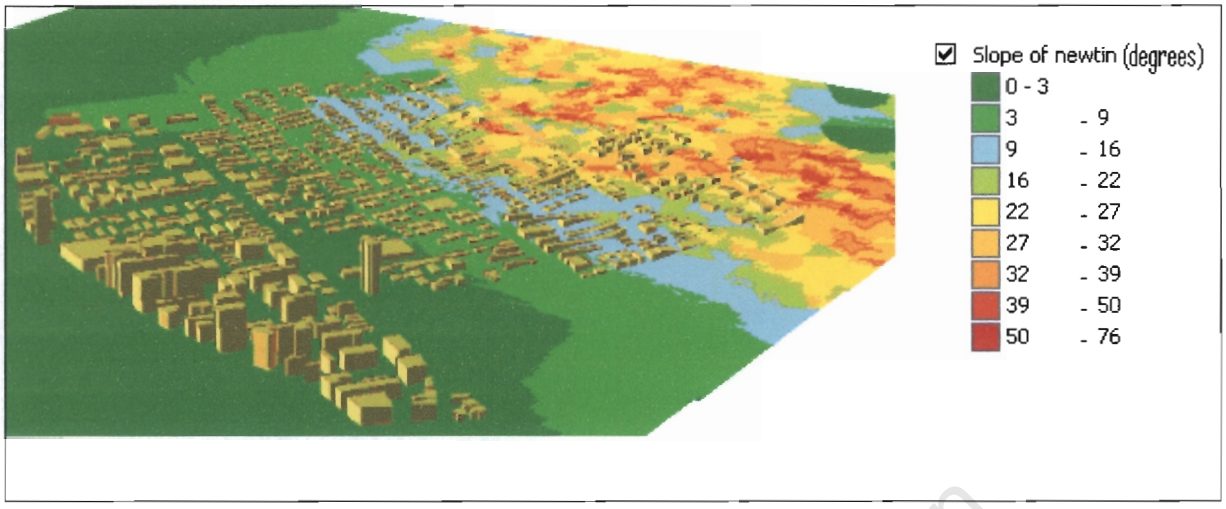

Figure 6.12: Slope map

Figure 6.13 shows a slope map of the area of study. Analysis of figure 6.13 and 6.12 shows some interesting relationships; the beach properties (beachprops) and the flat land properties (flatlandprops) have a slope of 0 – 3.9 degrees. Properties build on such a slope can be assumed to be on flat land. Therefore, the views of the properties behind the beach properties are very small due to obstruction. Gentle slope properties in figure 6.12 have a slope of 3.9-9.9 degrees on the slope map. Lower mountain properties (lowermntprops) in figure 6.12 have a slope of 9.9-16.2 degrees on the slope map.

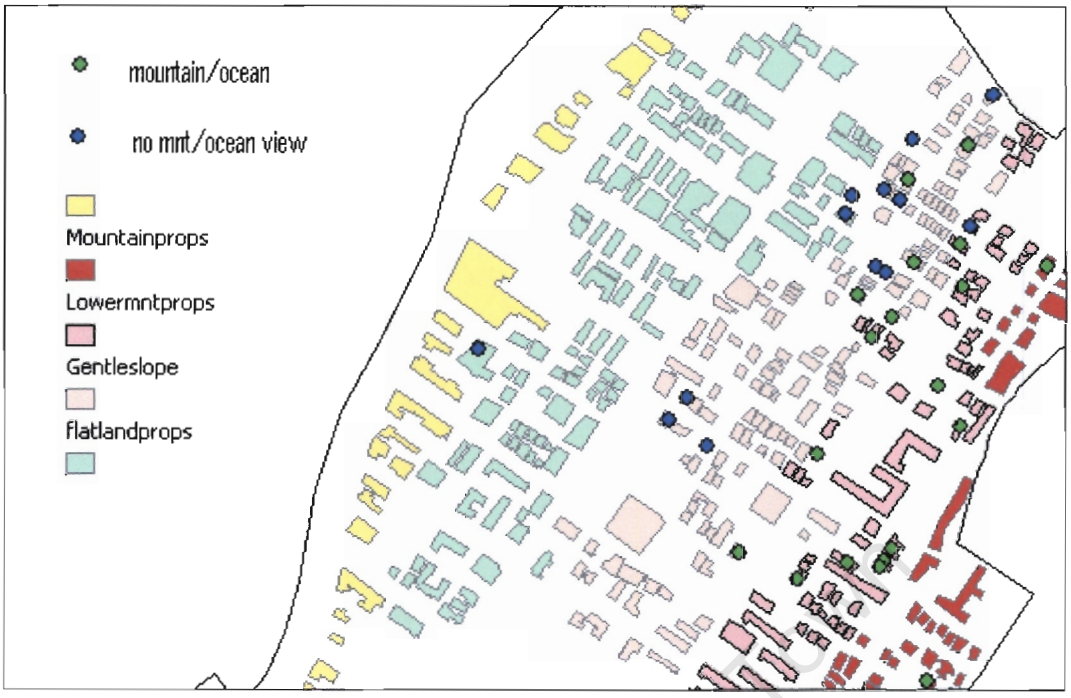

Figure 6.13: Types of views

Figure 6.13 shows properties with mountain and ocean views as well as those without mountain and ocean views. Properties with mountain and ocean views are mainly concentrated up the mountain. However, one finds properties with mountain and ocean down the mountain, in areas where the majority of the properties have neither ocean nor mountain views.

Table 6.5 summarises the relationships between the slope and the view observed.

Table 6.5: Slope and view factor relationship

View factor	Slope (degrees)	Description
<0.4	0-3.9	Flat land properties
0.4-0.5	3.9-9.9	Gentle slope properties
0.5-0.6	9.9-16.2	Lower mountain properties
0.6-0.8	16.2-39	Upper mountain properties
0.8-1	0-3.9	Beach front properties

6.9: Testing the results in CAMA

The view factors generated were exported into NCSS for CAMA analysis. The Cape Town quartile 4 model was used for the analysis. A new column was created in the data used by NCSS to accommodate the new view factors. The other model factors were unchanged and the same transformation procedure used during the GV2000 was followed.

NCSS Data - [C:\Documents and Settings\JKahonde\My Documents\Data\Qtl 4\thesis.S0]

File Edit Data Analysis Graphics PASS Window Help

PARCEL_YEAR

	Name	Label	Transformation	Format	Data Type	Value Label
215	ExpMultModel		EXP(MULTMODEL)			
216	LogResidRSA		LN(ResidRSA)			
217	COMBOMOD		ADDMODEL*ExpMultModel			
218	COMBOASR		COMBOMOD/SPRICE			
219	CalcAddMod		393.9848*RATEABLE_EXT+ 1742.23*TotLivArea+ 13195.13*TOTFIX3+ 188.900			
220	CalcMultMod		1.158839E-02*SALMON+ .9891441*LogQ4VWLV+ .6070239*LOGTestRsp+ .922			
221	ExpMult		EXP(CalcMultMod)			
222	CalcComboMod		CalcAddMod*ExpMult			
223	LogRSAHi		LN(RSAHiVar)			
224	LogQual		LN(Q4QUALLV)			
225	LogCond		LN(Q4CONDLV)			
226	GrannyFlat		sum(GRNYFLAT,D_GRNYFLAT)			
227	GFTLA		sum(TLA,(.5*d_finarea),GrannyFlat,(.8*SERVQTR),(.8*D_SERVQTR))			
228	ResidRSA					
229	zscore		MAX(.01,(SALETLA-4595)/2324+1)			
230	ReCalcGF		FILE(C:\CapeTown Models\QTL4\QTL4FinModGF.txt)			
231	FinVal2000		FILE(C:\CapeTown Models\QTL4\QTL4FinModGF.txt)			
232	C232					
233	View_linked		Lookup(parcel_ID,Prop_ID,view2,1)			
234	JustineViews		FILE(C:\Documents and Settings\Justine\Desktop\Qtl 4\viewModel.txt)			
235	Finalnoview		FILE(C:\Documents and Settings\JKahonde\My Documents\Data\Qtl 4\noview.t			
236	C236					
237	Sales2					
238	myview					
239	Mymodel		FILE(C:\Documents and Settings\JKahonde\My Documents\De			
240	C240					
241	C241					

Figure 6.14: Variable and transformation table

Figure 6.14 shows a snapshot of the variable and transformation table in NCSS. The variable name is entered in the first column, and its transformation is entered in the transformation column. The transformation is the mathematical formulae that represent the values of the variables.

6.9.1 Running the model

After the variables and all the transformations were set up, the model was run so as to calculate the new estimated property prices with the new view factors on. The complete table of results is shown in appendix A.

Table 6.6: Estimated prices

PID	Sales	Estimate	Ratio
CCT0000098	750000	733309.34	0.977746
CCT0000104	695000	850223.215	1.223343
CCT0000129	525000	506392.672	0.964557
CCT0000132	440000	678410.577	1.541842
CCT0000142	350000	296254.828	0.846442
CCT0000144	450000	528049.935	1.173444
CCT0000144	450000	575046.76	1.277882
CCT0000152	370000	491195.884	1.327556
CCT0000155	270000	263560.151	0.976149
CCT0000159	400000	440794.51	1.101986
CCT0000161	275000	438296.263	1.593805
CCT0000162	975000	1261220.37	1.293559
CCT0000165	340000	396764.89	1.166956
CCT0000169	820000		0
CCT0000170	584000	492809.905	0.843853
CCT0000171	432500	452360.704	1.045921
CCT0000173	335000	353514.049	1.055266
CCT0000175	820000	835955.051	1.019457
CCT0000177	495000	818759.409	1.654059
CCT0000178	390000	321791.893	0.825107
CCT0000180	425000	590370.159	1.389106
CCT0000184	560000	535466.472	0.95619
CCT0000187	730000	869511.42	1.191112
CCT0000193	180000	273335.83	1.518532
CCT0000195	475000	534243.493	1.124723
CCT0000199	540000	1265967.61	2.344384
CCT0000200	500000		0
CCT0000202	430000	655255.151	1.523849
CCT0000206	400000	576246.405	1.440616
CCT0000208	365000	753747.296	2.065061
CCT0000212	435000	390925.487	0.898679
CCT0000213	555000	659838.516	1.188898
CCT0000223	660000	566048.613	0.857649
CCT0000225	600000	750255.808	1.250426
CCT0000226	300000	481634.669	1.605449
CCT0000227	500000	496633.58	0.993267
CCT0000229	270000	359218.012	1.330437
CCT0000230	540000	685217.716	1.268922
CCT0000234	326500	484302.212	1.483315
CCT0000238	350000	622303.018	1.778009
CCT0000240	465000	504001.42	1.083874
CCT0000241	95126	2176616.92	22.88141
CCT0000247	1410000	1582793.86	1.122549

CCT0000249	1150000	1181362.03	1.027271
CCT0000251	1600000	1599428.27	0.999643
CCT0000259	525000	504998.568	0.961902
CCT0000260	1362500	1499912.98	1.100854
CCT0000261	430000	496983.992	1.155777
CCT0000261	430000	468139.906	1.088697
CCT0000263	450000	369770.768	0.821713
CCT0000265	480000	506152.371	1.054484
CCT0000268	950000	994013.588	1.04633
CCT0000278	380000	1456446.7	3.832754
CCT0000280	560000	1140877.07	2.03728
CCT0000281	660000	580497.858	0.879542
CCT0000284	620000	777844.94	1.254589
CCT0000285	1140000	995219.49	0.873
CCT0000287	1200000	1661198.49	1.384332
CCT0000289	120000	372314.059	3.102617
CCT0000291	644000	949731.66	1.474739
CCT0000294	272000	438762.768	1.613098
CCT0000351	1300000		0
CCT0000351	1300000	1288159.55	0.990892
CCT0000357	715000	1564678.34	2.188361
CCT0000362	1125000	1118120.97	0.993885
CCT0000372	1600000	1858553.15	1.161596
CCT0000383	2275000	2369827.24	1.041682
CCT0000384	644500	1097832.27	1.703386
CCT0000387	830000	867547.012	1.045237
CCT0000415	645000	552721.972	0.856933
CCT0000416	295000	488401.659	1.655599
CCT0000425	1100000	860089.958	0.7819
CCT0000430	144899	608444.985	4.199097
CCT0000444	870000	1050385.4	1.20734
CCT0092530	385000	461710.623	1.199248
CCT0129304	1100000	1268028.37	1.152753
CCT0129308	1075000	1185155.02	1.10247
CCT0129475	925000	1042910.99	1.127471
CCT0129760	345000	421826.273	1.222685
CCT0129763	332500	368671.852	1.108788
CCT0130487	500000	814607.294	1.629215
CCT0130665	490000	475266.738	0.969932
CCT0130970	220000	741103.427	3.368652
CCT0131574	397500	423683.657	1.065871
CCT0131625	501000	675599.686	1.348502
CCT0131630	550000	513031.825	0.932785
CCT0131663	350000	577743.746	1.650696
CCT0131709	700000	810129.966	1.157329
CCT0131798	231000	254454.238	1.101533
CCT0131987	380000	396275.571	1.04283
CCT0132009	795000		0
CCT0132034	375000	389370.99	1.038323

Table 6.6 shows the results of the model. It shows the Sales column against the estimated price from the model as well as the property identity (PID). In order to do a quick analysis of the results, a sales ratio is performed by dividing the estimated price by the sales price. For a good estimate, the ratio should be close to 1, that is, the estimated value should be approximately equal to the sale price. From table 6.7, it can be seen that the model over-estimated the majority of the property prices as evidenced by ratios which are more than 1. The majority of these properties are concentrated up the mountain. The over-estimation can be attributed to the fact that the roofs were not modelled thereby effectively reducing the obstruction to view.

Properties in the flat area with obstruction behaved as expected in that they did not exhibit great views. Most of these properties were modelled accurately. Their ratios were very close to 1.

6.9.2 Coefficient of determination *(R^2)*

As explained in chapter three, R^2 is the percentage of the variation in the sales prices explained by the regression model. It also ranges from 0 to 1.

Using equation 3.8:

$$R^2 = \sum\left(\hat{S}_i - \overline{S}\right)^2 / \sum\left(S_i - \overline{S}\right)^2 \qquad 3.8$$

R^2 was calculated to be **0.52**

The value of R^2 is much less than 1. It therefore implies that the majority of the variation in sales price cannot be explained by the regression model. Only about 52% of the variation in sales prices is explained by the model.

6.9.3 Standard error of estimate *(see)*

The standard error of estimate (see) measures the amount of deviation between the sale price and the estimated market value. Recalling equation 3.10:

$$see = \left[\sum \left(S_i - \hat{S}_i\right)^2 /(n - p - 1)\right]^{1/2}$$

The calculate ***see*** was R 416 889.77. According to Eckert, (1990), if the errors are normally distributed, then:

- 66% of the sale prices should fall within one *see* of their estimated values
- 95% of the sale prices should fall within two *see* of their estimated values, and
- 99% of the sale prices should fall within three *see* of their estimated values

Table 6.7: Analysis of *see*

One see (R 416 889)	Two see (R 833 778)	Three see (R1 250 667)
30%	80%	94%

From table 6.7, it is clear that only 30% of the sale prices fall within one *see*, 80% fall within two *see*, and 94% fall within three *see*. It therefore means that the errors in the model are not normally distributed.

6.9.4 Coefficient of Variation *(CoV)*

CoV is *see* expressed as a percentage of the average sale price and multiplied by 100. Recalling equation 3.11:

$$CoV = (100 * see / \bar{S})$$

$$= (100*416890)/610194$$

$$= 68\%$$

This implies that, given a normal distribution, roughly two-thirds of sales prices lie within 68 percent of their predicted values. However, it has been shown in the evaluation of *see* that the normal distribution condition is not met in this case. Therefore, the interpretation of CoV is meaningless in this regard.

CHAPTER SEVEN: CONCLUSIONS AND RECOMMENDATIONS

7.1 Introduction

This chapter summarises and provides a synthesis of conclusions of the methods used to model view and the application in CAMA. In Chapter One the author introduced this study with the objective of developing an automated method of measuring view using GIS and 2.5-D modelling for the purposes of CAMA modelling which is more accurate than the existing inspection methods. The objectives and hypotheses of this study were subsequently posited. In the literature review in Chapter Two, the author introduced the reader to the existing methods of determining view and the level to which GIS has been used in the determination of view for CAMA methods. The literature review revealed that the determination of view in the CAMA realm is shifting towards the use of advanced GIS techniques such as 2.5-D modelling (Yu et al., 2004). In Chapter Three, the GIS theory pertinent to this research work was explained. It was seen that a DTM was central to the modelling of view using GIS techniques. Different data structures used to represent a DTM were discussed and the pros and cons highlighted. The viewshed analysis found within the ESRI product ArcGIS 9 was the tool used to simulate and analyse the view. Chapter Four saw the development of the conceptual design of the view model. The main focus here was the analysis of the error in the view model. To that end, error propagation techniques were applied and several scenarios were considered. In Chapter Five the methodology is explained, while Chapter Six focused on presenting the results and their analyses.

In this final Chapter, a summary of the methods used to develop the view model is made. From the summary, the author draws conclusions to the general theory, the validity of the hypothesis as well as the research questions and finally areas of further research.

7.2 Conceptual Design

During the conceptual design stage, the author derived ways of quantifying the error in the observation angles given the error in the surface models. Several scenarios were considered and the corresponding error in view was determined. The aim of this chapter was to provide the relative errors in view associated with different sizes of the raster cells used to create the grid DTM.

7.3 Results and Analysis

The results and analysis section dealt with DTM modelling using the TIN method and the raster DTM method from contour data, the modelling of the buildings and the generation of the combined model of the terrain and the buildings. The viewshed analysis was performed on the combined surface, and the view factors were subsequently generated. The view factors were then exported into NCSS for CAMA analysis.

7.3.1 DTM modelling

In this research work, two DTMs were produced from the contour data. The first DTM was produced using the TIN method and the second was produced using the raster method.

The Delaunay triangulation technique was used to generate the TIN, while the sequential steepest slope technique was used to generate the raster DTM from the contours. The main purpose of generating the TIN model was to carry out the visualisation analysis. This type of analysis helps to check the accuracy of the DTM visually by ensuring that peculiar features can be identified on the DTM (Naser, et al., 2005). The results confirmed the theory that a TIN model gives the best surface representation. In this case, mountain peaks were modelled precisely by the TIN. The steepest sequential slope method was used to generate the raster DTM using a grid size of 1m by 1m. The accuracy of the TIN was compared with the accuracy of the raster DTM. The TIN proved to be of higher accuracy than the DTM. This result also confirmed that the accuracy of the DTM depends on the size of the cell.

7.3.2 Buildings modelling

Buildings were generated from footprints extracted from the aerial photographs. The aerial photograph rectified to remove errors during the time of photography. Therefore, the accuracy of the aerial photographs was assumed to be high. Digitising errors were assessed by overlaying the footprints on top of the erven. The assumption here was that the erven were accurate. The footprints were extruded by their height to generate the building model. The buildings were then converted into raster format.

7.3.3 Combined model

The combined model of the DTM and the buildings was generated by adding corresponding cells on the DTM and on the building model. The buildings footprints were overlaid on top to assess the error introduced by converting the buildings into raster format.

7.4 Viewshed analysis

Two observers were chosen for every building within the study area, one facing the ocean and the other facing the mountain. Viewshed analysis was performed and the results were analysed by dividing the number of visible cells by the number of cells for the best views. The results showed that the properties can be classified into five different groups according to the view they exhibited. Properties along the beach exhibited the best views followed by properties high on the mountains which enjoyed wide panoramic views. Properties on the flat ground and in the middle of the suburb exhibited poor views.

7.5 CAMA analysis

The model used for the Cape Town Quartile 4 modelling region was adopted for this research work. This was to allow for comparison between the results with new view factors and the results with the old factors. The results of this research work showed R^2 of 52% compared to the GV2000 model which gave R^2 of 75%. The poor results can be attributed to the fact that the terrain model did not include trees and roofs.

7.6 Analysis of the hypotheses

The objective of this study was develop an automated method of determining view factors for the purposes of CAMA modelling using 2.5-D modelling and GIS. The hypotheses that were posited were to establish:

(a) If GIS and 2.5-D modelling could be used to in CAMA modelling in order to develop an automated process of determining more accurate view data.

From the above hypotheses, three research questions were formulated:

(1) **What other methods can one use to determine view for the purposes of CAMA modelling?**

From the literature review it was shown that the main method used in many parts of the world is the inspection method (Bourassa, et al., 2003). GIS was being used by some jurisdictions at the level of spatial analysis.

(2) **Can the process of determining view be automated in order to improve on efficiency of determination of the impact of view on property values, to reduce the element of subjectivity, and to improve the time and cost effectiveness of determining this characteristic?**

According to the findings of this study, many techniques need to be put in place in setting up the model before the view analysis can be performed. Critical to this development is the generation of the relevant terrain surfaces on which view analysis can be performed. The generation of the terrain and the buildings require high levels of accuracy to ensure that the determination of view is also accurate. Many factors affect the accuracy of the surface models as explained in Chapter Four. Once the relevant surfaces have been modelled, the process of carrying view analysis is automatic. However, many viewshed maps are generated and good file organisation is needed in order to maintain the data. Since the method of generating the view factors depends on the properties with the best view, subjectivity is eliminated because every viewshed is divided by the same number representing the best view. The properties

exhibited view qualities that are related to their topography. Once everything has been set up, the procedure can be performed much faster than the manual inspection method currently applied. For metropolitan cities such as the City of Cape Town, this procedure is very cost effective because they already have the relevant software and personnel required to run the system. In house training is encouraged to make sure that the people who run the system are fully aware of the techniques required. The answer to the research question is positive.

(3) **Do the automated methods produce better models for the purposes of CAMA modelling?**

The answer to the above question is no. According to this study, the automated method did not produce better models for the purposes of CAMA modelling. The poor model can be attributed to low accuracy spatial data used to generate the terrain models. However, with improvement in the accuracy of the data used for the generation of view factors, it is thought that the view factors themselves could be significantly improved which would lead to more acceptable CAMA outputs.

7.7 Recommendations for further research

From the findings of this research, the author concludes that it is possible to use GIS and 2.5D modelling to determine view for the purposes of CAMA analysis. However, more accurate methods of generating DTMs should be found as this is thought to be the primary limitation of the technique. To that end, the use of LASER scanning techniques and LIDAR techniques, as well as digital photogrammetry is recommended in order to generate a realistic model of obstructions that better models building shapes, includes their roofs, and includes other obstructions such as vegetation. This is expected to improve the accuracy of the view factors, and lead to better results from the CAMA modelling.

With an improved obstructions model, the research could also be extended to include a larger test area, such as the entire area encompassed by Quartile 4 in the GV2000 Project. In this manner a comparison between the modelling results would demonstrate only the difference in the methods of modelling view, and would not be related to sample size.

The author also recommends that tools like Model builder and Python be used in further research to automate the process and to perform the viewshed indices calculation.

7.8 Conclusions

This study has shown that GIS and 2.5D modelling can be used to automate the determination of view for the purposes of CAMA modelling. The author has used secondary GIS data to generate the terrain models and to run the viewshed analysis. Two terrain surfaces were generated using the TIN method and the raster method. The TIN method proved to be more accurate than the raster method. Buildings were modelled from the aerial photographs and were combined with the DTM to generate a combined model on which viewshed analysis was performed. The results of the viewshed analysis enabled the properties to be grouped into five different categories depending on the type of view observed. It was also found out that the categorisation also showed some correlation with the slope. This research has also shown that the data used to generate the model does not give better results in terms of CAMA modelling. From the findings of this research, the City of Cape Town stands to benefit in the long run if it decides to build upon the method developed by taking into consideration the recommendations posited.

REFERENCES

Baldwin, J., Darling, A., Correll, M.R. (1998), "The effect of Environmental Amenities on House Values: The example of a View Lot, *Professional Geographer*, Vol 33, 216-220.

Benson, E.D., Hansen, L.J., Schwartz, A.L., Smersh, G.T. (1998), "Pricing Amenities: The Value of View." *Journal of Real Estate Finance and Economics*, Vol 16, pp.55 -73.

Bond, M.T., Seiler, V.L, Seiler M.J. (2002), "Residential Real Estate Prices: A Room with a View", *Journal of Real Estate Research*, Vol 23, 129-137.

Bourassa, S.C., Hoesli, M., Sun. J. (2003), "What's in a View?" *Working Paper. Paper presented at 8th Asian Real Estate Society International Conference, 25-28 August, Singapore.*

Chen, Z.T., and Tobler, W., (1986), "Quadtree representations of digital terrain," *Proceedings of Auto-Carto Conference, 22-24 May*, London.

Davis, J., (1986), "Statistics and Data Analysis in Geology," New York, John Wiley & Sons.

Eckert, J.K. (1990), "Property Administration and Assessment Administration", *International Association of Assessing Officers, Chicago.*

Fisher, P.F. (1993), "Algorithm and Implementation uncertainty in Viewshed analysis", *International Journal of Geographical Information Systems*, Vol 7, pp. 331 – 374.

French, N., Pagourtzi, E., Assimakopoulos, V. and Hatzichristos, T. (2003), "Real Estate Appraisal: A Review of Valuation Methods", *Journal of Property Investment and Finance*, Vol. 21, No. 4, pp. 383 – 401.

Gloudemans, R.J (1999), "Mass Appraisal of Real Property", International Association Of Assessing Officers, Chicago.

Jahne, B., (1997), "Digital Image Processing: Concepts, Algorithms, and Scientific Applications," Berlin, Applied Science Publishers.

Kennie, T.J.M. and Petrie, G. (1990), "Engineering Surveying Technology", J. Wiley & Sons.

Kulshreshtha, S.N. and Gilles, J.A. (1993), "Economic Evaluation of Aesthetic Amenities: A Case Study of River View". *Water Resources Bulletin*, Vol 29, pp. 257 – 266.

Lake, I.R., Lovett, A.A., Bateman, I.J., Langford, I.H. (1998), "Modelling Environmental Influences on Property Prices in an Urban Environment". *Computers, Environment and Urban Systems*, Vol 22, pp. 121 – 136.

Leberl, F. and Oslon, D. (1982), "Raster scanning for operational digitising of graphical data," *Photogrammetric Engineering and Remote Sensing*, Vol 48(4), pp. 615 – 627.

McCluskey, W.J. and Borst, R.A. (1997), "An Evaluation of MRA, Comparable Sales Analysis and ANNs for the Mass Appraisal of Residential Properties in Northern Ireland", *Assessment Journal*, Vol. 4, No. 1, pp. 47 – 58.

McCullagh, M.J., and Ross, C.G., (1980), "Delaunay triangulation of a random data set for isarithmic mapping," *The Cartographic Journal*, Vol 17(2), pp.93 – 99.

Naser, E., Valeo, C., and Habib, A., (2005), "Digital Terrain Modeling," London, John Wiley & Sons.

Optech Inc., (2002), "Optech – Laser Based Ranging, Mapping and Detection Systems.
http://www.optech.on.ca Last Accessed on August 2005.

Paterson, R.W., Boyle, K.J. (2002), "Out of Sight, Out of Mind? Using GIS to Incorporate Visibility in Hedonic Property Value Models", *Land Economics*, Vol 78(3), pp. 417-425.

Rana, S. and Morley, J. (2002), "Optimising Visibility Analyses Using Topographic Features on the Terrain". *Working Paper, Centre for Advanced Spatial Analysis*, paper 44.

Samet, H., (1984), "The quadtree and related data structures," *ACM Computing Surveys,* Vol 16(2), pp. 187 – 260.

Seiler, M.J., Bond, M.T., Seiler, V.L. (2001), "The Impact of World Class Great Lakes Water Views on Residential Property Values", *Appraisal Journal*, Vol 69(3), pp. 287 – 295.

Shears, J.C., and Allan, J.W., (1996), "Softcopy photogrammetry and its uses in GIS," *ESRI User Conference, 26-29 March, Palm Springs, CA*.

Tucker, G.E., and Slingerland, R.L., (1997), "Drainage basin response to climate change," *Water Resources Research*, Vol 33(8), pp. 2031 – 2047.

Ward, R.W.(2001), "Demonstration of CAMA in South Africa", *Assessment Journal*, Vol. 8, No. 3, pp. 33 – 43.

Wehr, A., and Lohr, U., (1999), "Airborne laser scanning: an introduction and overview," *ISPRS Journal of Photogrammetry & Remote Sensing*, Vol (54), pp. 68 – 82.

Whittal, J., (2006), "View Error Analysis", *Unpublished Notes*.

Yu, S., Han, S., and Chai, C. (2004), "Modeling the Value of View in Real Estate Valuation: A 3-D GIS Approach", *working paper presented at PRRES conference, 16-19 December, Beijing.*

BIBLIOGRAPHY

Bjorke, J.T., (1988), "Quadtrees and triangulation in digital elevation models," *International Archives of Photogrammetry and Remote Sensing, International Society for Photogrammetry and Remote Sensing, Committee of the 16th International Congress of ISPRS*, Vol (27), pp.38 – 44.

Clark, I., (1979), "Practical Geostatistics," London, Applied Science Publishers.

ESRI (1992), "ArcGIS 3D Analyst: Three Dimensional Visualisation, Topographic Analysis and Surface Creation", *ESRI White Papers*, [On-line] Available: http://www.esri.com/library/whitepapers/ Last accessed in February 2005.

ESRI (2002, January), "ArcGIS 3D Analyst: Three Dimensional Visualisation, Topographic Analysis and Surface Creation", *ESRI White Papers*, [On-line] Available: http://www.esri.com/library/whitepapers/arcgisxt_lit.html#whitepapers Last accessed in June 2005.

Hu, Y., Xue, Y., Fang, K., and Pan, Z., (1999), "Scanning laser altimeter in airborne scanning laser ranging-image sensor," *Proceedings of the Fourth International Airborne Remote Sensing Conference and Exhibition*, Canadian Symposium on Remote Sensing, Ottawa, Canada, Vol (1), pp. 510 – 517.

APPENDIX A: VIEW FACTORS AND THE ESTIMATED PRICES

Sales (R)	Estimated Price (R)	PID	View index
750000	733309.3398	CCT0000098	0.16
695000	850223.2146	CCT0000104	0.11
525000	506392.6721	CCT0000129	0.16
440000	678410.5767	CCT0000132	0.35
350000	296254.828	CCT0000142	0.35
450000	528049.9354	CCT0000144	0.22
450000	575046.7603	CCT0000144	0.34
370000	491195.8844	CCT0000152	0.48
270000	263560.1511	CCT0000155	0.40
400000	440794.5096	CCT0000159	0.20
275000	438296.2626	CCT0000161	0.32
975000	1261220.373	CCT0000162	0.99
340000	396764.8901	CCT0000165	0.30
820000		CCT0000169	0.40
584000	492809.9045	CCT0000170	0.25
432500	452360.7042	CCT0000171	0.36
335000	353514.0494	CCT0000173	0.42
820000	835955.0514	CCT0000175	0.73
495000	818759.4086	CCT0000177	0.16
390000	321791.8932	CCT0000178	0.36
425000	590370.1593	CCT0000180	0.21
560000	535466.4724	CCT0000184	0.16
730000	869511.4196	CCT0000187	0.26
180000	273335.8304	CCT0000193	0.32
475000	534243.4927	CCT0000195	0.23
540000	1265967.605	CCT0000199	0.16
500000		CCT0000200	0.83
430000	655255.1506	CCT0000202	0.15
400000	576246.4047	CCT0000206	0.23
365000	753747.2957	CCT0000208	0.84
435000	390925.4874	CCT0000212	0.41
555000	659838.5157	CCT0000213	0.50
660000	566048.6125	CCT0000223	0.22
600000	750255.8082	CCT0000225	0.79
300000	481634.6692	CCT0000226	0.22
500000	496633.58	CCT0000227	0.20
270000	359218.0115	CCT0000229	0.41
540000	685217.7158	CCT0000230	0.79
326500	484302.2121	CCT0000234	0.40
350000	622303.0181	CCT0000238	0.46
465000	504001.4203	CCT0000240	1.10
95126	2176616.915	CCT0000241	0.84
1410000	1582793.855	CCT0000247	0.76
1150000	1181362.03	CCT0000249	0.65
1600000	1599428.272	CCT0000251	0.57
525000	504998.5683	CCT0000259	0.49
1362500	1499912.984	CCT0000260	0.91
430000	496983.9923	CCT0000261	0.31

430000	468139.9057	CCT0000261	0.31
450000	369770.7675	CCT0000263	0.21
480000	506152.3714	CCT0000265	0.65
950000	994013.5882	CCT0000268	0.25
380000	1456446.699	CCT0000278	0.76
560000	1140877.068	CCT0000280	0.49
660000	580497.8575	CCT0000281	0.99
620000	777844.9402	CCT0000284	0.25
1140000	995219.4904	CCT0000285	0.63
1200000	1661198.487	CCT0000287	0.41
120000	372314.0587	CCT0000289	0.22
644000	949731.6601	CCT0000291	0.15
272000	438762.7676	CCT0000294	0.36
1300000		CCT0000351	0.49
1300000	1288159.549	CCT0000351	0.71
715000	1564678.338	CCT0000357	0.37
1125000	1118120.968	CCT0000362	0.21
1600000	1858553.148	CCT0000372	0.53
2275000	2369827.239	CCT0000383	0.77
644500	1097832.273	CCT0000384	0.41
830000	867547.0124	CCT0000387	0.20
645000	552721.9718	CCT0000415	0.21
295000	488401.6589	CCT0000416	0.31
1100000	860089.9582	CCT0000425	0.37
144899	608444.9854	CCT0000430	0.20
870000	1050385.402	CCT0000444	0.46
385000	461710.6229	CCT0092530	0.75
1100000	1268028.372	CCT0129304	0.58
1075000	1185155.022	CCT0129308	0.83
925000	1042910.99	CCT0129475	0.48
345000	421826.2728	CCT0129760	0.14
332500	368671.8518	CCT0129763	0.49
500000	814607.2936	CCT0130487	0.21
490000	475266.7376	CCT0130665	0.22
220000	741103.4271	CCT0130970	0.20
397500	423683.657	CCT0131574	0.15
501000	675599.6861	CCT0131625	0.15
550000	513031.8253	CCT0131630	0.35
350000	577743.7457	CCT0131663	0.11
700000	810129.966	CCT0131709	0.31
231000	254454.2384	CCT0131798	0.20
380000	396275.5705	CCT0131987	0.15
795000		CCT0132009	0.30
375000	389370.9902	CCT0132034	0.36
	1424777.461	CCT0132171	0.71

APPENDIX B: BUILDING HEIGHT INFORMATION

Bldheight (m)	Prop_ID
3	CCT0132178
3	CCT0132180
3	CCT0132179
3	CCT0131722
3	CCT0131724
3	CCT0131723
6	CCT0131994
3	CCT0131729
3	CCT0131728
3	CCT0131697
3	CCT0131726
3	CCT0131727
3	CCT0131885
6	CCT0131695
3	CCT0131688
3	CCT0131987
3	CCT0131694
3	CCT0131698
3	CCT0000144
6	CCT0131696
3	CCT0131689
3	CCT0131718
3	CCT0000129
6	CCT0130665
3	CCT0131705
3	CCT0131936
3	CCT0131703
3	CCT0131701
3	CCT0131700
3	CCT0000142
3	CCT0129763
3	CCT0129760
3	CCT0129759
15	CCT0129758
3	CCT0129757
3	CCT0130846
3	CCT0131652
3	CCT0131640
6	CCT0131975
3	CCT0131650
6	CCT0131999
6	CCT0131910
3	CCT0131661

3	CCT0132175
6	CCT0131647
3	CCT0132138
9	CCT0000200
3	CCT0131646
3	CCT0000175
3	
3	CCT0131681
3	CCT0131672
3	CCT0131970
6	CCT0131642
3	CCT0131643
3	CCT0131645
6	CCT0131644
6	CCT0131641
3	CCT0131983
3	
3	CCT0131651
3	CCT0131682
3	CCT0131680
3	
3	CCT0131678
3	CCT0131677
3	CCT0131676
3	CCT0131675
3	CCT0131662
3	CCT0131673
3	CCT0091883
3	CCT0000189
3	CCT0000184
3	CCT0131684
3	CCT0131671
3	CCT0131670

APPENDIX C: SALES CLEANING

PID	DATE	SALE (R)	X (Lo19/84)	Y (Lo19/84)	TLA (m^2)	ERFEXT (m^2)	GOOD
CCT0000098	2000/02/14	750000.00	-56251.89	-3755015.77	151.00	**396.00**	**1**
CCT0000104	2000/02/15	695000.00	-56529.21	-3755035.67	151.00	**401.00**	**1**
CCT0000129	1999/02/10	525000.00	-55872.08	-3753958.57	181.00	**396.00**	**1**
CCT0000132	1999/10/22	440000.00	-55684.00	-3753994.77	146.00	**566.00**	**1**
CCT0000142	2000/02/09	350000.00	-55974.14	-3754015.04	122.00	**201.00**	**1**
CCT0000144	2000/08/24	450000.00	-55900.76	-3754023.17	149.00	**664.00**	**1**
CCT0000152	1999/08/25	370000.00	-55979.89	-3754068.41	101.00	**221.00**	**1**
CCT0000154	1999/04/29	930000.00	-55618.54	-3754081.86	201.00	**498.00**	**1**
CCT0000155	2000/03/17	270000.00	-56010.50	-3754079.38	84.00	**167.00**	**1**
CCT0000159	1999/08/27	400000.00	-56052.41	-3754088.64	166.00	**178.00**	**1**
CCT0000161	1999/04/08	275000.00	-55990.50	-3754093.15	169.00	**265.00**	**1**
CCT0000162	1999/01/14	975000.00	-55707.46	-3754104.16	156.00	**551.00**	**1**
CCT0000164	1999/06/24	890000.00	-55614.21	-3754114.93	294.00	**478.00**	**1**
CCT0000165	2000/01/20	340000.00	-56060.41	-3754111.83	162.00	**138.00**	**1**
CCT0000169	2000/02/10	820000.00	-55677.57	-3754128.85	0.00	**538.00**	**3**
CCT0000170	1999/11/30	584000.00	-55899.21	-3754127.38	149.00	**377.00**	**1**
CCT0000171	1999/06/24	432500.00	-55688.54	-3754137.68	115.00	**264.00**	**1**
CCT0000173	2000/03/09	335000.00	-55913.35	-3754150.79	77.00	**110.00**	**1**
CCT0000175	2000/02/23	820000.00	-55801.24	-3754177.84	170.00	**545.00**	**1**
CCT0000177	1999/05/14	495000.00	-55972.92	-3754172.64	143.00	**131.00**	**1**
CCT0000178	1999/11/05	390000.00	-56023.08	-3754178.79	83.00	**147.00**	**1**
CCT0000180	1999/01/28	425000.00	-56007.62	-3754186.50	170.00	**203.00**	**1**
CCT0000184	1999/10/20	560000.00	-55908.95	-3754203.61	180.00	**277.00**	**1**
CCT0000187	1999/11/05	730000.00	-56044.41	-3754214.81	274.00	**430.00**	**1**
CCT0000189	1999/05/14	888000.00	-55895.79	-3754212.80	202.00	**226.00**	**1**
CCT0000193	2000/01/24	180000.00	-56002.24	-3754244.85	61.00	**103.00**	**1**
CCT0000195	1999/08/25	475000.00	-56028.36	-3754269.40	156.00	**318.00**	**1**
CCT0000199	1999/10/08	540000.00	-56537.36	-3754285.44	206.00	**446.00**	**1**
CCT0000200	1999/09/13	500000.00	-55940.09	-3754333.36	0.00	**405.00**	**3**
CCT0000202	2000/04/11	430000.00	-56265.63	-3754347.38	162.00	**401.00**	**1**
CCT0000208	1999/04/19	365000.00	-55913.07	-3754385.19	124.00	**592.00**	**1**
CCT0000212	2000/01/27	435000.00	-56239.50	-3754409.17	158.00	**379.00**	**1**
CCT0000213	1999/08/17	555000.00	-56095.50	-3754420.71	208.00	**311.00**	**1**
CCT0000223	1999/02/21	660000.00	-56617.83	-3754506.59	127.00	**258.00**	**1**
CCT0000225	1999/05/22	600000.00	-56002.25	-3754542.84	152.00	**218.00**	**1**
CCT0000226	1999/12/03	300000.00	-56199.06	-3754547.21	93.00	**151.00**	**1**
CCT0000227	1999/10/14	500000.00	-56011.73	-3754557.42	113.00	**222.00**	**1**
CCT0000229	1999/08/16	270000.00	-56058.46	-3754559.85	67.00	**100.00**	**1**
CCT0000230	1999/02/25	540000.00	-56016.58	-3754564.90	142.00	**223.00**	**1**
CCT0000234	1999/10/15	326500.00	-56122.77	-3754581.94	101.00	**130.00**	**1**
CCT0000238	1999/02/05	350000.00	-56383.86	-3754686.94	132.00	**264.00**	**1**
CCT0000240	1999/12/31	465000.00	-56363.17	-3754701.71	113.00	**292.00**	**1**
CCT0000241	1999/10/01	95126.00	-55957.74	-3754712.87	238.00	**751.00**	**3**
CCT0000247	1999/10/08	1410000.00	-56037.17	-3754733.23	304.00	**446.00**	**1**
CCT0000249	2000/02/23	1150000.00	-56037.26	-3754759.82	271.00	**694.00**	**1**
CCT0000251	1999/08/20	1600000.00	-56069.23	-3754786.75	292.00	**614.00**	**1**
CCT0000259	2000/03/16	525000.00	-56214.82	-3754828.96	116.00	**194.00**	**1**

CCT0000260	1999/09/25	1362500.00	-55990.62	-3754833.64	328.00	**689.00**	**1**
CCT0000261	2000/11/07	360000.00	-56209.45	-3754832.56	124.00	**182.00**	**1**
CCT0000263	1999/03/04	450000.00	-56264.15	-3754834.27	108.00	**163.00**	**1**
CCT0000265	1999/10/24	480000.00	-56247.47	-3754845.63	108.00	**190.00**	**1**
CCT0000268	1999/04/30	950000.00	-56299.11	-3754866.88	291.00	**669.00**	**1**
CCT0000278	1999/09/15	380000.00	-56229.96	-3754913.06	125.00	**372.00**	**1**
CCT0000280	2000/01/30	560000.00	-56616.01	-3754922.83	187.00	**302.00**	**1**
CCT0000281	1999/10/22	660000.00	-56214.26	-3754923.55	167.00	**372.00**	**1**
CCT0000284	1999/07/16	620000.00	-56572.41	-3754948.07	158.00	**309.00**	**1**
CCT0000285	2000/03/02	1140000.00	-56209.50	-3754950.40	165.00	**372.00**	**1**
CCT0000287	1999/05/14	1200000.00	-56606.44	-3754956.79	293.00	**626.00**	**1**
CCT0000289	1999/06/30	120000.00	-56247.11	-3754954.38	68.00	**119.00**	**3**
CCT0000291	1999/10/15	644000.00	-56590.14	-3754966.23	181.00	**626.00**	**1**
CCT0000294	1999/03/31	272000.00	-56253.11	-3754974.77	88.00	**162.00**	**1**
CCT0000351	2000/09/07	1300000.00	-57392.88	-3755211.86	360.00	**868.00**	**3**
CCT0000357	1999/07/27	715000.00	-57366.96	-3755235.87	316.00	**471.00**	**1**
CCT0000362	1999/12/23	1125000.00	-56339.96	-3755253.04	250.00	**447.00**	**1**
CCT0000372	1999/06/23	1600000.00	-56139.70	-3755285.46	268.00	**596.00**	**1**
CCT0000383	2000/01/05	2275000.00	-56201.65	-3755325.59	364.00	**514.00**	**1**
CCT0000384	1999/06/14	644500.00	-57307.85	-3755343.92	222.00	**639.00**	**1**
CCT0000387	2000/02/07	830000.00	-57164.59	-3755368.84	167.00	**456.00**	**1**
CCT0000415	2000/03/06	645000.00	-57105.68	-3755443.22	95.00	**229.00**	**3**
CCT0000416	1999/03/02	295000.00	-57066.64	-3755442.81	101.00	**159.00**	**1**
CCT0000425	1999/07/23	1100000.00	-57196.18	-3755479.65	195.00	**449.00**	**1**
CCT0000430	1999/03/26	144899.00	-57316.47	-3755474.89	154.00	**136.00**	**3**
CCT0000444	1999/05/03	870000.00	-57165.07	-3755515.35	181.00	**544.00**	**1**
CCT0033743	1999/02/09	520000.00	0.00	0.00	135.00	**529.00**	**1**
CCT0034937	2000/05/02	385000.00	-56532.26	-3754764.33	154.00	**847.00**	**1**
CCT0034960	2000/08/16	370000.00	-56522.27	-3754749.48	162.00	**119.00**	**1**
CCT0034987	2000/06/19	385000.00	-56525.63	-3754754.35	154.00	**115.00**	**1**
CCT0092530	2000/08/29	385000.00	-56168.54	-3754817.90	85.00	**277.00**	**1**
CCT0129304	2000/06/01	1100000.00	-56350.93	-3755204.04	180.00	**559.00**	**1**
CCT0129308	2000/05/08	1075000.00	-56358.38	-3755216.85	178.00	**559.00**	**1**
CCT0129475	2000/10/19	925000.00	-56514.99	-3755011.12	189.00	**401.00**	**1**
CCT0129760	2000/06/15	345000.00	-55972.01	-3753992.36	127.00	**498.00**	**1**
CCT0129763	2000/03/30	332500.00	-55993.61	-3754001.57	116.00	**192.00**	**1**
CCT0130487	1999/11/16	500000.00	-56537.18	-3754975.47	204.00	**316.00**	**1**
CCT0130665	2000/06/12	490000.00	-55918.96	-3753972.90	170.00	**489.00**	**1**
CCT0130970	2000/08/01	220000.00	-57042.14	-3755446.47	208.00	**518.00**	**3**
CCT0131574	2000/08/04	397500.00	-56151.11	-3754871.63	115.00	**246.00**	**1**
CCT0131625	2000/04/23	501000.00	-56258.15	-3754490.53	181.00	**425.00**	**1**
CCT0131630	2000/07/07	550000.00	-56235.53	-3754522.17	136.00	**234.00**	**1**
CCT0131663	2000/07/12	350000.00	-56147.13	-3754188.65	264.00	**370.00**	**1**
CCT0131709	2000/06/24	700000.00	-56060.28	-3754259.58	188.00	**888.00**	**1**
CCT0131987	2000/08/08	380000.00	-55874.47	-3754008.25	75.00	**156.00**	**1**
CCT0132034	2000/07/27	375000.00	-56253.38	-3754950.19	70.00	**120.00**	**1**
CCT0132171	2000/10/18	0.00	-55638.79	-3754236.89	239.00	**428.00**	**3**

APPENDIX D: VISIBLE CELLS

			VISIBLE CELLS		
PID	X (Lo19/84)	Y (Lo19/84)	Ocean	Mountain	Average
CCT0000098	-56252	-3755016			34231
CCT0000104	-56529	-3755036		23415	
CCT0000129	-55872	-3753959			33896
CCT0000132	-55684	-3753995		74321	
CCT0000142	-55974	-3754015			73421
CCT0000144	-55901	-3754023			46983
CCT0000144	-55901	-3754023		72314	
CCT0000152	-55980	-3754068		101234	
CCT0000155	-56011	-3754079			85644
CCT0000159	-56052	-3754089			42461
CCT0000161	-55991	-3754093			67462
CCT0000162	-55707	-3754104	164532	44987	
CCT0000165	-56060	-3754112			64326
CCT0000169	-55678	-3754129		84563	
CCT0000170	-55899	-3754127			53876
CCT0000171	-55689	-3754138		75648	
CCT0000173	-55913	-3754151		89607	
CCT0000175	-55801	-3754178	133245	22364	
CCT0000177	-55973	-3754173		34568	
CCT0000178	-56023	-3754179			75834
CCT0000180	-56008	-3754187			44890
CCT0000184	-55909	-3754204		33546	
CCT0000187	-56044	-3754215		54372	
CCT0000193	-56002	-3754245		67543	
CCT0000195	-56028	-3754269		49854	
CCT0000199	-56537	-3754285			34532
CCT0000200	-55940	-3754333	132896	43456	
CCT0000202	-56266	-3754347			32896
CCT0000206	-56289	-3754377			48562
CCT0000208	-55913	-3754385	98753	78654	
CCT0000212	-56240	-3754409			87465
CCT0000213	-56096	-3754421	105321		
CCT0000223	-56618	-3754507			46891
CCT0000225	-56002	-3754543	134576	32456	
CCT0000226	-56199	-3754547		45736	
CCT0000227	-56012	-3754557		43275	
CCT0000229	-56058	-3754560		87564	
CCT0000230	-56017	-3754565	124573	43234	
CCT0000234	-56123	-3754582		85432	
CCT0000238	-56384	-3754687		98453	
CCT0000240	-56363	-3754702	202345	32123	
CCT0000241	-55958	-3754713	112358	66754	
CCT0000247	-56037	-3754733	105439	55687	
CCT0000249	-56037	-3754760	104342	33245	
CCT0000251	-56069	-3754787	87564	33245	
CCT0000259	-56215	-3754829	104986		
CCT0000260	-55991	-3754834	102999	89675	

CCT0000261	-56209	-3754833			**64879**
CCT0000261	-56209	-3754833		**65432**	
CCT0000263	-56264	-3754834			**43768**
CCT0000265	-56247	-3754846	**138563**		
CCT0000268	-56299	-3754867			**53987**
CCT0000278	-56230	-3754913	**101239**	**59834**	
CCT0000280	-56616	-3754923		**103587**	
CCT0000281	-56214	-3754924	**134256**	**76645**	
CCT0000284	-56572	-3754948			**53861**
CCT0000285	-56210	-3754950	**110453**	**23512**	
CCT0000287	-56606	-3754957		**87645**	
CCT0000289	-56247	-3754954			**47342**
CCT0000291	-56590	-3754966		**32175**	
CCT0000294	-56253	-3754975		**76543**	
CCT0000351	-57393	-3755212	**104563**		
CCT0000351	-57393	-3755212	**105397**	**45362**	
CCT0000357	-57367	-3755236	**79453**		
CCT0000362	-56340	-3755253		**45634**	
CCT0000372	-56140	-3755285	**80342**	**33289**	
CCT0000383	-56202	-3755326	**134279**	**28976**	
CCT0000384	-57308	-3755344	**86546**		
CCT0000387	-57165	-3755369			**43123**
CCT0000415	-57106	-3755443		**44362**	
CCT0000416	-57067	-3755443		**65432**	
CCT0000425	-57196	-3755480			**78956**
CCT0000430	-57316	-3755475			**43234**
CCT0000444	-57165	-3755515	**98765**		
CCT0092530	-56169	-3754818	**124572**	**33745**	
CCT0129304	-56351	-3755204	**99854**	**23123**	
CCT0129308	-56358	-3755217	**100285**	**76854**	
CCT0129475	-56515	-3755011		**102394**	
CCT0129760	-55972	-3753992		**28745**	
CCT0129763	-55994	-3754002	**103456**		
CCT0130487	-56537	-3754975		**45634**	
CCT0130665	-55919	-3753973			**46315**
CCT0130970	-57042	-3755446			**43213**
CCT0131574	-56151	-3754872		**32456**	
CCT0131625	-56258	-3754491			**32129**
CCT0131630	-56236	-3754522		**74563**	
CCT0131663	-56147	-3754189			**22957**
CCT0131709	-56060	-3754260		**65434**	
CCT0131798	-56029	-3754227			**42145**
CCT0131987	-55874	-3754008		**32456**	
CCT0132009	-56257	-3754919		**64345**	
CCT0132034	-56253	-3754950		**76543**	
CCT0132171	-55639	-3754237	**116573**	**33456**	